

Experimental Tests of Asymptotic Freedom

S. Bethke

Max-Planck-Institut für Physik, Munich, Germany

February 5, 2008

Abstract

Quantum Chromodynamics (QCD), the gauge field theory of the Strong Interaction, has specific features, asymptotic freedom and confinement, which determine the behaviour of quarks and gluons in particle reactions at high and at low energy scales. QCD predicts that the strong coupling strength α_s decreases with increasing energy or momentum transfer, and vanishes at asymptotically high energies. In this review, the history and the status of experimental tests of asymptotic freedom are summarised. The world summary of measurements of α_s is updated, leading to an unambiguous verification of the running of α_s and of asymptotic freedom, in excellent agreement with the predictions of QCD. Averaging a set of measurements balanced between different particle processes and the available energy range, results in a new and improved world average of $\alpha_s(M_{Z^0}) = 0.1189 \pm 0.0010$.

MPP-2006-54
June 2006

arXiv:hep-ex/0606035v2 15 Jun 2006

Contents

1	Introduction	3
2	Historical Development	4
2.1	A New Force	4
2.2	Quarks	4
2.3	Chromo-Dynamics	5
2.4	Asymptotic Freedom	5
2.5	Scaling Violations	6
2.6	Quark and gluon jets in high energy collisions	6
2.7	Status in the late 1980's	7
3	Theoretical Basis	9
3.1	Renormalization	9
3.2	α_s and its energy dependence	10
3.3	Asymptotic freedom and confinement	10
3.4	The running coupling	11
3.5	Relative size of finite order approximations	12
3.6	Quark masses and thresholds	13
3.7	Perturbative predictions of physical quantities	14
3.8	Renormalization scale dependence.	15
3.9	Nonperturbative QCD methods	16
4	Tests of Asymptotic freedom in e^+e^- annihilations	16
4.1	Jet production rates	17
4.2	Evidence for the gluon self coupling	19
4.3	Determination of the QCD group constants	20
4.4	The running α_s from 4-jet event production	20
5	QCD tests in deep inelastic lepton-nucleon scattering	22
5.1	Basic introduction to structure functions	22
5.2	Scaling violations of structure functions	23
5.3	The running α_s from jet production in DIS	24
6	Summary of α_s measurements	25
6.1	Previous developments and current status	25
6.2	Update: new results since 2004	26
6.3	α_s summary	27
6.4	A new world average of $\alpha_s(M_{Z^0})$	30
7	Summary and Outlook	31

1 Introduction

The Strong Interaction, binding quarks and gluons inside hadrons, is the strongest of the four fundamental forces in nature which we know today. It is about 100 times stronger than the electromagnetic force, a factor of 10^{14} stronger than the Weak Interaction, and a stunning factor of 10^{40} stronger¹ than the Gravitational Force, calculated for two quarks at a distance of order 1 fm.

In spite of these differences, it is the Gravitational and the Electromagnetic Forces which seem to play the dominating role in the universe which we experience in the macroscopic world. The reason for this wondrous fact is that the Strong Force, as well as the Weak Interaction, only acts at subatomic distances. Taking the existence of atomic nuclei, their composition and their masses for granted, restricting ourselves to energies and temperatures below 1 MeV and, respectively, 10^8 Kelvin, the Strong Interaction is disguised in the description of the world.

At subatomic distances, however, this picture changes completely. The Strong Force not only determines the binding of quarks and gluons inside hadrons, it also determines the cohesion of protons and neutrons inside atomic nuclei. Hadrons like protons and neutrons are responsible for more than 99% of the mass of all visible matter in our universe, and those masses are mainly generated by the strong binding of quarks inside hadrons, rather than by the (generally small) masses of the quarks themselves.

The restriction of the Strong Force to subatomic distances is a consequence of two characteristic features: they are called “Confinement” and “Asymptotic Freedom”.

Confinement is a necessary requirement to explain the fact that no isolated quarks have ever been observed in any experiment, although symmetry arguments and scattering experiments in the 1960’s established quarks, with $-1/3$ or $+2/3$ of electrical charge units and a newly introduced quantum property called “colour charge”, as the basic constituents of hadrons. Confinement determines that at large distances, or - equivalently - at low momentum or energy transfer in elementary particle reactions, the Strong Force prevents the existence of free quarks: Trying to separate two quarks from each other, for instance in high energy scattering reactions, apparently results in an increase of the force field’s energy at large distances, such that new quarks are created out of the vacuum - the initial quarks “dress” up with other quarks to build hadrons. These hadrons exhibit no net colour charge to the outside, such that they appear as elementary entities rather than the quarks themselves².

The term “Asymptotic Freedom” is used to describe the behaviour of quarks at high energy or momentum transfers, or - equivalently - at small distances. Also this feature is based on experimental observations: In high energy scattering processes between leptons (e.g. electrons or neutrinos) with protons or neutrons, the dynamics reveal that scattering occurs at pointlike and massless constituents, the quarks, rather than at a homogenous object with the size of a proton. Apparently, at sufficiently high momentum transfers, quarks behave like free or weakly bound particles. Also, quarks knocked out of a hadron, in a high energy scattering process, were never observed as free particles. Instead, they emerge as dressed-up hadrons or bundles (jets) of hadrons escaping from the interaction region.

The fact that the strong interaction becomes “weak” at high energy scales, and vanishes to zero at asymptotically high energies, led to the term “Asymptotic Freedom”. Any theory describing and predicting the dynamics of quarks inside hadrons and in high energy reactions therefore had to satisfy and include these two extremes: Confinement, also called “infrared slavery”, and Asymptotic Freedom.

A theoretical description of the Strong Interaction by a consistent quantum field theory, called Quantum Chromodynamics (QCD), was presented in 1972 by Fritzsche and Gell-Mann [1], which was formally published later in [2]. At the same time it was found by Gross, Politzer and Wilczek that non-Abelian gauge theories, such as QCD, exhibit the property of Asymptotic Freedom [3]. This discovery was honored with the Nobel Prize in 2004, 30 years after the original findings.

¹40 orders of magnitude correspond to the difference in size of our entire universe to the size of an atomic nucleus.

²Van-der-Vaals-like remnant forces bind protons and neutrons in atomic nuclei.

Theoretical breakthroughs and discoveries, before being honored by the Nobel Prize, must be established by experimental measurements. The price for Asymptotic Freedom therefore also had to await experimental verification. In this article, the long but exciting road to experimental evidence for Asymptotic Freedom shall be summarised.

2 Historical Development

2.1 A New Force

In the 1930's, protons and Neutrons were recognised as the building blocks of atomic nuclei. A new and elementary force, the so-called Strong Force, was introduced phenomenologically, in order to explain the binding of these particles inside nuclei. These binding energies were known to be much larger than what could be expected from the well-known electromagnetic force. Also, the electromagnetic force was known to have infinite range while the Strong Force apparently acted only within nuclear distances of the order of femtometer.

Shortly after these perceptions, Hideki Yukawa argued that the range of the electromagnetic force was infinite because the associated exchange particle, the photon, was massless, and proposed that the short range of the strong force was due to the exchange of a massive particle which was called "meson" [4]. From quantum mechanical arguments and from Heisenberg's uncertainty principle Yukawa predicted a meson mass³ of about $100 \text{ MeV}/c^2$. At that time, no particle with a mass in that range was known.

Very soon after, in 1937, a new particle was discovered whose mass was very close to that of Yukawa's prediction of the meson - however, this particle in fact was the muon which turned out not to be subject to the strong interaction. Finally, in 1947 strongly interacting particles with masses close to Yukawa's prediction were found [5] in emulsion experiments at high altitudes. A particle which met Yukawa's requirements was found, and it was called "pion". Although today we know that pions, like protons and neutrons, are composite particles made from quarks, and the Strong Interaction is not mediated through the exchange of pions, Yukawa's theory stimulated major advances in the understanding and description of the strong interaction.

2.2 Quarks

In the decades after World War II, the number of strongly interacting particles exploded - which was basically due to the development of particle accelerators with steadily increasing energies. Strongly interacting particles were then called "hadrons", which differentiate into mesons (with integer or zero spins) and baryons (with spins of $1/2$ or $3/2$). Gell-Mann and Zweig realised in 1964 that the whole spectroscopy of hadrons could be explained by a small number of "quarks" if baryons are made out of 3 quarks, and mesons out of one quark plus one antiquark [6]. Those quarks, initially 3 different species, then must have $1/3$ or $2/3$ of the elementary charge unit, and they must have spin $1/2$.

By the end of the 1960's, the static picture of quarks as the constituents of hadrons was confirmed through the dynamics observed at high energy electron-proton scattering experiments at the Stanford Linear Accelerator (SLAC)[7], summarised in figure 1: the cross sections - instead of decreasing with increasing momentum transfer as expected for elastic scattering of electrons at protons as a whole - showed a "scaling" behaviour, as it should occur if the electrons scatter on quasi-free, pointlike and nearly massless constituents inside the protons.

While the quark model was very successful in describing the properties, multitude and dynamic behaviour of hadrons, it had severe shortcomings such as an obvious violation of the Pauli-principle

³From now on, in this review, a system of units is utilized where the speed of light and Planck's constant are set to unity, $c = \hbar = 1$, such that energies, momenta and masses are all given in units of eV.

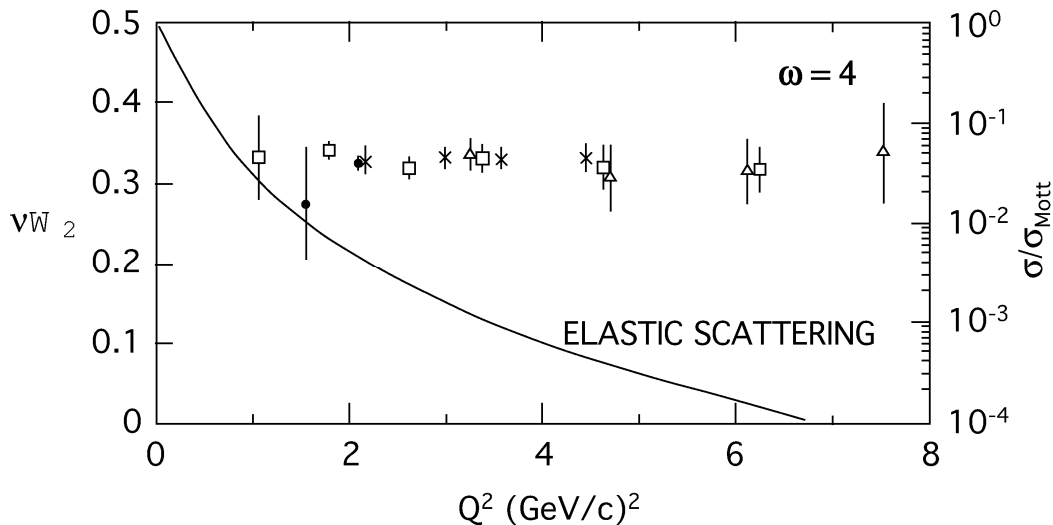


Figure 1: The structure function of the proton, describing the electron- proton scattering in units of the Mott cross section, i.e. the generalised Rutherford cross section at high energies, as measured at SLAC [7]. $\omega = 4$ corresponds to $x = 0.25$ in figure 13.

for hadrons containing two or three identical quarks in relative S-waves and in identical spin states, the prediction of the neutral pion’s lifetime which was wrong by a factor of nine, and the fact that no particles (quarks) with $1/3$ or $2/3$ of the elementary charge unit could ever be observed at particle colliders.

2.3 Chromo-Dynamics

To overcome these shortcomings, the idea that the strong force couples to a new quantum property, called colour charge [8, 9], in analogy to the photon in QED which couples to the electric charges.

The introduction of the new quantum number, describing 3 different colour quantum states of each of the quark species, solved the puzzle of spin-statistics, saved the Pauli-principle and explained the missing factor of nine ($= 3^2$) of the pion lifetime. The notion that hadrons consist either of three quarks (baryons like the proton) or a quark and an antiquark (mesons), arranged such that the net color charge of the hadron would vanish - i.e. “white” as a superposition of the three elementary color states or of a particular color and its anti-color - could account for the fact that the strong force is short-ranged.

Finally, in the early 1970’s, a field theory of the strong force, Quantum Chromodynamics (QCD), was introduced and presented in canonical form [1, 2]. Here, coloured spin-1 particles called “gluons”, which - in contrast to the case of photons in QED - carry colour charge themselves, couple to the colour charges of quarks, and also to coloured gluons themselves. Chromo-Statics turned into Chromo-Dynamics.

2.4 Asymptotic Freedom

A few years before, it was demonstrated in model theories that charges may change their effective size when they are probed in scattering experiments, at large and at small distances. These changes were described through Symanzik’s β -function [10], see equation 2 below: the effective size of the coupling strength is a function of the energy or momentum transfer, Q^2 . The SLAC data on approximate scaling of the proton structure function, c.f. figure 1, and the notion of free quarks inside the proton required a negative β -function. At that time, however, all field theories probed so far had a positive β -function.

Gross, Politzer and Wilczek finally demonstrated in 1973 that Chromo-Dynamics, with coloured quarks and gluons, obeying $SU(3)_{colour}$ symmetry, generated a negative β -function [3], i.e. that quarks and gluons are asymptotically free. This explained the SLAC data, and at the same time leads - for small momentum transfers or at large distances, to an increase of the coupling strength, thus motivating confinement.

Another important consequence from asymptotic freedom is the fact that the strong coupling α_s is small enough, at sufficiently large momentum transfers, to allow application of perturbation theory in order to provide quantitative predictions of physical processes.

With this discovery Quantum Chromodynamics started its triumphal procession as being *the* field theory of the strong interaction. It was, however, a long and difficult path before QCD was commonly accepted to be exactly that. Many refined calculations, theoretical predictions and experimental verifications were ventured. The most important features of QCD, asymptotic freedom and/or, equivalently, the existence of colour charged gluons, had to be tested, quantified and “proven” by experiment. The size of the strong coupling parameter, $\alpha_s(Q^2)$, had to be determined and its energy dependence verified to be compatible with asymptotic freedom.

2.5 Scaling Violations

The violation of approximate scaling of the proton structure function was one of the first experimental signatures proposed to test QCD [11]. Deep inelastic electron-proton (or more generally, lepton-nucleon) scattering processes basically depend on two kinematical parameters. The usual choice of these parameters are the momentum transfer Q^2 between the lepton and the struck quark, and the fraction x of the proton’s momentum which is carried by the struck quark.

The structure function F_2 of the proton basically parametrises the population of quarks with momentum fraction x , as a function of Q^2 : $F_2(x, Q^2)$. QCD predicts that the region of large x is depopulated for higher momentum transfers, while the population at low x should increase with increasing Q^2 .

A simple argument for this behaviour can be given in terms of the equivalence of momentum transfer and physical resolution: with higher Q^2 , smaller distances are probed. At smaller distances, an increased radiation of soft (low energy) gluons should be resolved. These gluons increase the population of partons at small x , and - at the same time - diminish the momentum fraction and the relative contribution of quarks at large x .

On top of it’s kinematical origin, scaling violations in x and Q^2 are modified by the specific energy dependence of the strong coupling. Note that a qualitative observation of scaling violations of structure functions alone does not yet prove Asymptotic Freedom - such a conclusion requires a large lever arm in Q^2 and a precise study of the functional form of observed scaling violations, as e.g. the logarithmic slopes, $\partial F_2(x, Q^2)/\partial \ln Q^2$.

While scaling violations were already observed in the 1970’s, initially it was not possible to conclude that asymptotic freedom was actually seen [12, 13]. Instead, unknown higher order QCD terms, the effects of target masses and nonperturbative effects (“higher twists”) could cause similar effects as those predicted by asymptotic freedom. Only with the availability of much higher Q^2 and the ability to probe much smaller values of x , e.g. at the electron-proton collider HERA, stricter conclusions were possible in the past 10 to 15 years. These will be presented in more detail in section 5.

2.6 Quark and gluon jets in high energy collisions

Another class of predictions, basically governed by the concept of confinement, was the expectation of collimated hadron jets in high energy reactions like $e^+e^- \rightarrow q\bar{q}$ [14, 15]. Indeed, by 1975, the emergence of 2-jet structure was observed when increasing the e^+e^- center of mass energy E_{cm} from 3 to 7.4 GeV [16], confirming the basic ideas of the quark-parton model.

The radiation of energetic gluons off high energetic quarks was predicted from QCD, and hence the emergence of a third hadron jet was expected in e^+e^- annihilation at higher energies [17]. In 1979, 3-jet structures were observed at the PETRA e^+e^- collider at $E_{cm} \approx 30$ GeV [18], see figure 2. The 3rd jet could be attributed to the emission of a third parton with zero electric charge and spin 1 [19] – the gluon was discovered and explicitly seen!

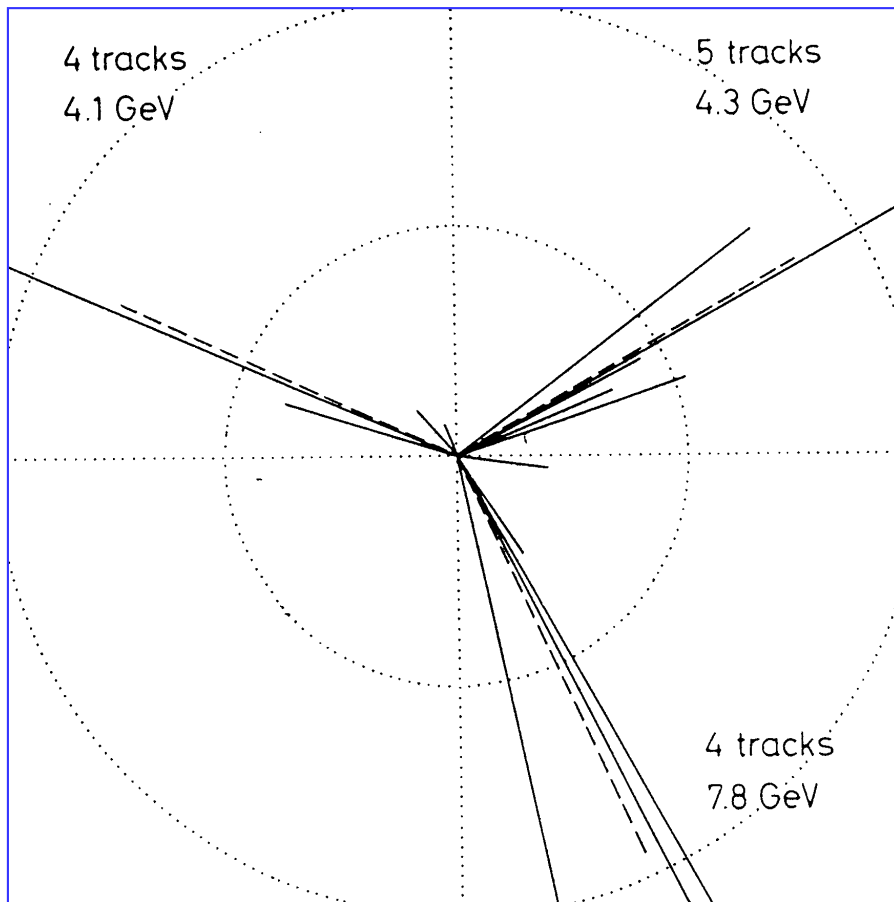


Figure 2: The first 3-jet event, observed by the TASSO experiment at the PETRA e^+e^- storage ring [18].

After an almost parameter-free description of hadronic event shapes [20, 21] had served to establish gluon radiation beyond any doubts, first determinations of the coupling strength α_s were performed. More detailed studies of the jet structure and the shape of hadronic events provided insights into the color structure of the gluon, like for instance the “string effect” [22] which was expected in QCD due to the higher color charge of the gluon [23].

2.7 Status in the late 1980’s

Towards the end of the 1980’s, after successful exploitation of the experimental programs of the e^+e^- storage rings PETRA at DESY and PEP at SLAC, the proton-antiproton collider at CERN and many deep inelastic lepton-nucleon experiments at CERN, at Fermilab and at SLAC, “*the experimental support for QCD is quite solid and quantitative*” [24], however convincing *proofs* of the key features of QCD, of the gluon-selfcoupling and/or of asymptotic freedom, were still not available. As an example, the summary of measurements of α_s at different energy scales in 1989, as reproduced in figure 3 [24],

was compatible with the QCD expectation of the running of α_s , but did not yet allow to draw more concrete conclusions.

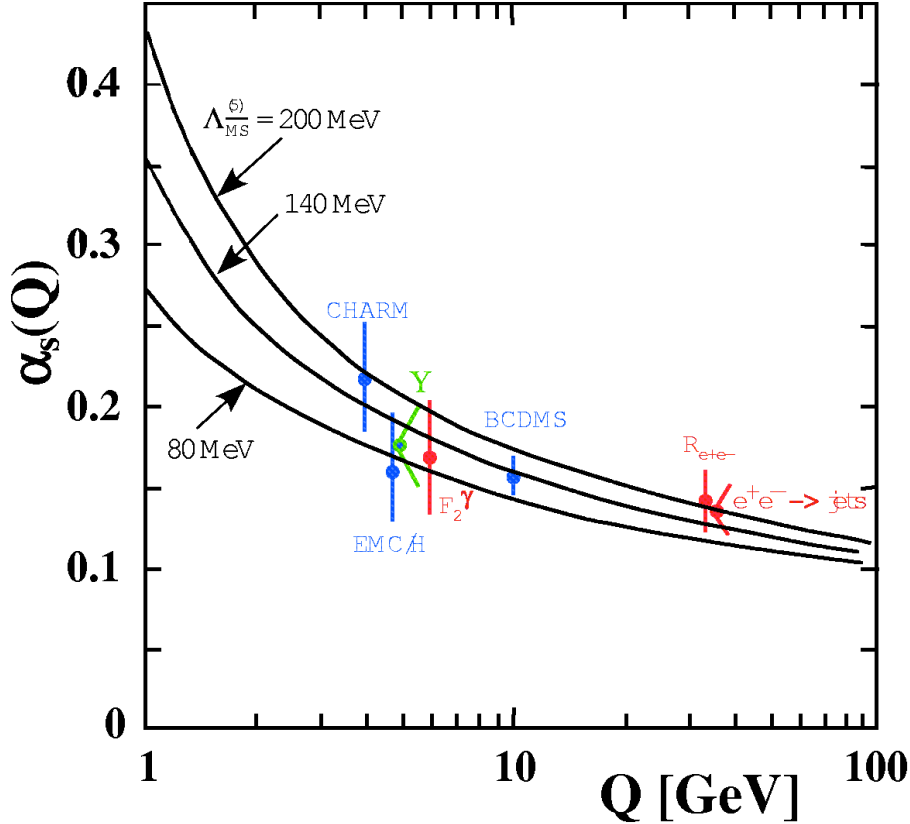


Figure 3: Summary of measurements of α_s in 1989 [24]. Shown are results from various experiments in deep inelastic lepton-nucleon scattering as well as combined results from e^+e^- collisions, together with the QCD expectation of a running α_s for different values of $\Lambda_{\overline{MS}}$ (see section 3).

Foundations were laid, however, to prepare for more quantitative tests with the upcoming higher energy colliders, like the e^+e^- colliders LEP at CERN and SLC at SLAC, the Tevatron $p\bar{p}$ collider at Fermilab and the HERA electron-proton collider at DESY, who all started operation in the time from 1987 to 1991:

- From the summary of α_s measurements shown in figure 3, using the QCD prediction of a running coupling, the value of $\alpha_s(Q^2 = M_{Z^0}^2)$, at the energy scale of the Z^0 boson mass, $M_{Z^0} \approx 90$ GeV, was predicted to be $\alpha_s(M_{Z^0}) = 0.11 \pm 0.01$. Experiments at LEP and SLC were determined to scrutinise this prediction with high accuracy [24].
- Deep inelastic scattering results, extending to much higher values of Q^2 and much lower values of x , should prove scaling violations of nucleon structure functions.
- Significant progress in jet physics allowed to prepare for direct tests of asymptotic freedom, through the energy dependence of jet production rates [25, 26], and of the gluon-selfcoupling, through spin-correlations in 4-jet hadronic final states in e^+e^- annihilation [27].
- Precise determinations of α_s at low and at high energy scales, in e^+e^- annihilation, at hadron colliders and in deep inelastic lepton-nucleon collisions were expected to emerge, with the prospect of proving the energy dependence of α_s , and thus, asymptotic freedom.

- Theoretical developments like precise calculations in next-to-leading (NLO) and next-next-to-leading order (NNLO) perturbation theory, advanced methods of handling theoretical uncertainties, and improvement in the understanding of the nonperturbative hadronisation process, in terms of advanced Monte Carlo models, had started and were expected to be confronted with future high precision experimental data.

After a short summary of the theoretical basics of QCD in section 3, the developments of experimental test of QCD, and in particular of asymptotic freedom, following the status as summarised above, will be presented in more detail in sections 4 to 6.

3 Theoretical Basis

The concepts of QCD are portrayed in many text books and articles, se e.g. [28, 29, 30, 31, 32], and in particular, the article of G.M.Prosperi, M. Raciti and C.Simolo in this issue of PPNP [33]. In the following, a brief summary of the basics of perturbative QCD and of the energy dependent strong coupling parameter, α_s , is given.

3.1 Renormalization

In quantum field theories like Quantum Chromodynamics (QCD) and Quantum Electrodynamics (QED), physical quantities \mathcal{R} can be expressed by a perturbation series in powers of the coupling parameter α_s or α , respectively. If these couplings are sufficiently small, i.e. if $\alpha_s \ll 1$, the series may converge sufficiently quickly such that it provides a realistic prediction of \mathcal{R} even if only a limited number of perturbative orders will be known.

In QCD, examples of such quantities are cross sections, decay rates, jet production rates or hadronic event shapes. Consider \mathcal{R} being dimensionless and depending on α_s and on a single energy scale Q . This scale shall be larger than any other relevant, dimensional parameter such as quark masses. In the following, these masses are therefore set to zero.

When calculating \mathcal{R} as a perturbation series of a pointlike field theory in α_s , ultraviolet divergencies occur. These divergencies are removed by the “renormalisation” of a small set of physical parameters. Fixing these parameters at a given scale and absorbing this way the ultraviolet divergencies, introduces a second but artificial momentum or energy scale μ . As a consequence of this procedure, \mathcal{R} and α_s become functions of the renormalization scale μ . Since \mathcal{R} is dimensionless, we assume that it only depends on the ratio Q^2/μ^2 and on the renormalized coupling $\alpha_s(\mu^2)$:

$$\mathcal{R} \equiv \mathcal{R}(Q^2/\mu^2, \alpha_s); \quad \alpha_s \equiv \alpha_s(\mu^2).$$

Because the choice of μ is arbitrary, however, the actual value of the experimental observable \mathcal{R} cannot depend on μ , so that

$$\mu^2 \frac{d}{d\mu^2} \mathcal{R}(Q^2/\mu^2, \alpha_s) = \left(\mu^2 \frac{\partial}{\partial \mu^2} + \mu^2 \frac{\partial \alpha_s}{\partial \mu^2} \frac{\partial}{\partial \alpha_s} \right) \mathcal{R} \stackrel{!}{=} 0, \quad (1)$$

where the derivative is multiplied with μ^2 in order to keep the expression dimensionless. Equation 1 implies that any explicite dependence of \mathcal{R} on μ must be cancelled by an appropriate μ -dependence of α_s to all orders. It would therefore be natural to identify the renormalization scale with the physical energy scale of the process, $\mu^2 = Q^2$, eliminating the uncomfortable presence of a second and unspecified scale. In this case, α_s transforms to the “running coupling constant” $\alpha_s(Q^2)$, and the energy dependence of \mathcal{R} enters only through the energy dependence of $\alpha_s(Q^2)$.

Any residual μ -dependence is a measure of the quality of a given calculation in finite perturbative order.

3.2 α_s and its energy dependence

While QCD does not predict the absolute size of α_s , its energy dependence is precisely determined. If $\alpha_s(\mu^2)$ is measured at a given scale, QCD definitely predicts its size at any other energy scale Q^2 through the renormalization group equation

$$Q^2 \frac{\partial \alpha_s(Q^2)}{\partial Q^2} = \beta(\alpha_s(Q^2)) . \quad (2)$$

The perturbative expansion of the β function is calculated to complete 4-loop approximation [34]:

$$\beta(\alpha_s(Q^2)) = -\beta_0 \alpha_s^2(Q^2) - \beta_1 \alpha_s^3(Q^2) - \beta_2 \alpha_s^4(Q^2) - \beta_3 \alpha_s^5(Q^2) + \mathcal{O}(\alpha_s^6) , \quad (3)$$

where

$$\begin{aligned} \beta_0 &= \frac{33 - 2N_f}{12\pi} , \\ \beta_1 &= \frac{153 - 19N_f}{24\pi^2} , \\ \beta_2 &= \frac{77139 - 15099N_f + 325N_f^2}{3456\pi^3} , \\ \beta_3 &\approx \frac{29243 - 6946.3N_f + 405.089N_f^2 + 1.49931N_f^3}{256\pi^4} , \end{aligned} \quad (4)$$

and N_f is the number of active quark flavours at the energy scale Q . The numerical constants in equation 4 are functions of the group constants $C_A = N$ and $C_F = (N^2 - 1)/2N$, for theories exhibiting $SU(N)$ symmetry; for QCD and $SU(3)$, $C_A = 3$ and $C_F = 4/3$. β_0 and β_1 are independent of the renormalization scheme, while all higher order β coefficients are scheme dependent.

3.3 Asymptotic freedom and confinement

A solution of equation 2 in 1-loop approximation, i.e. neglecting β_1 and higher order terms, is

$$\alpha_s(Q^2) = \frac{\alpha_s(\mu^2)}{1 + \alpha_s(\mu^2)\beta_0 \ln \frac{Q^2}{\mu^2}} . \quad (5)$$

Apart from giving a relation between the values of α_s at two different energy scales Q^2 and μ^2 , equation 5 also demonstrates the property of asymptotic freedom: if Q^2 becomes large and β_0 is positive, i.e. if $N_f < 17$, $\alpha_s(Q^2)$ will asymptotically decrease to zero.

Likewise, equation 5 indicates that $\alpha_s(Q^2)$ grows to large values and, in this perturbative form, actually diverges to infinity at small Q^2 : for instance, with $\alpha_s(\mu^2 \equiv M_{Z^0}^2) = 0.12$ and for typical values of $N_f = 2 \dots 5$, $\alpha_s(Q^2)$ exceeds unity for $Q^2 \leq \mathcal{O}(100 \text{ MeV} \dots 1 \text{ GeV})$. Clearly, this is the region where perturbative expansions in α_s are not meaningful anymore, and we may regard energy scales below the order of 1 GeV as the nonperturbative region where confinement sets in, and where equations 2 and 5 cannot be applied.

Including β_1 and higher order terms, similar but more complicated relations for $\alpha_s(Q^2)$, as a function of $\alpha_s(\mu^2)$ and of $\ln \frac{Q^2}{\mu^2}$ as in equation 5, emerge. They can be solved numerically, such that for a given value of $\alpha_s(\mu^2)$, choosing a suitable reference scale like the mass of the Z^0 boson, $\mu = M_{Z^0}$, $\alpha_s(Q^2)$ can be accurately determined at any energy scale $Q^2 \geq 1 \text{ GeV}^2$.

If we set

$$\Lambda^2 = \frac{\mu^2}{e^{1/(\beta_0 \alpha_s(\mu^2))}} ,$$

a dimensional parameter Λ is introduced such that equation 5 transforms into

$$\alpha_s(Q^2) = \frac{1}{\beta_0 \ln(Q^2/\Lambda^2)} . \quad (6)$$

Hence, the Λ parameter is technically identical to the energy scale Q where $\alpha_s(Q^2)$ diverges to infinity, $\alpha_s(Q^2) \rightarrow \infty$ for $Q^2 \rightarrow \Lambda^2$. To give a numerical example, $\Lambda \approx 0.1$ GeV for $\alpha_s(M_{Z^0} \equiv 91.2 \text{ GeV}) = 0.12$ and $N_f = 5$.

The parametrization of the running coupling $\alpha_s(Q^2)$ with Λ instead of $\alpha_s(\mu^2)$ has become a common standard, see e.g. [31], and will also be adopted here. While being a convenient and well-used choice, however, this parametrization has several subtleties:

First, requiring that $\alpha_s(Q^2)$ must be continuous when crossing a quark threshold⁴, Λ actually depends on the number of active quark flavours. Secondly, Λ depends on the renormalization scheme, see e.g. reference [29]. In this review, the so-called ‘‘modified minimal subtraction scheme’’ ($\overline{\text{MS}}$) [35] will be adopted, which also has become a common standard [31]. Λ will therefore be labelled $\Lambda_{\overline{\text{MS}}}^{(N_f)}$ to indicate these peculiarities.

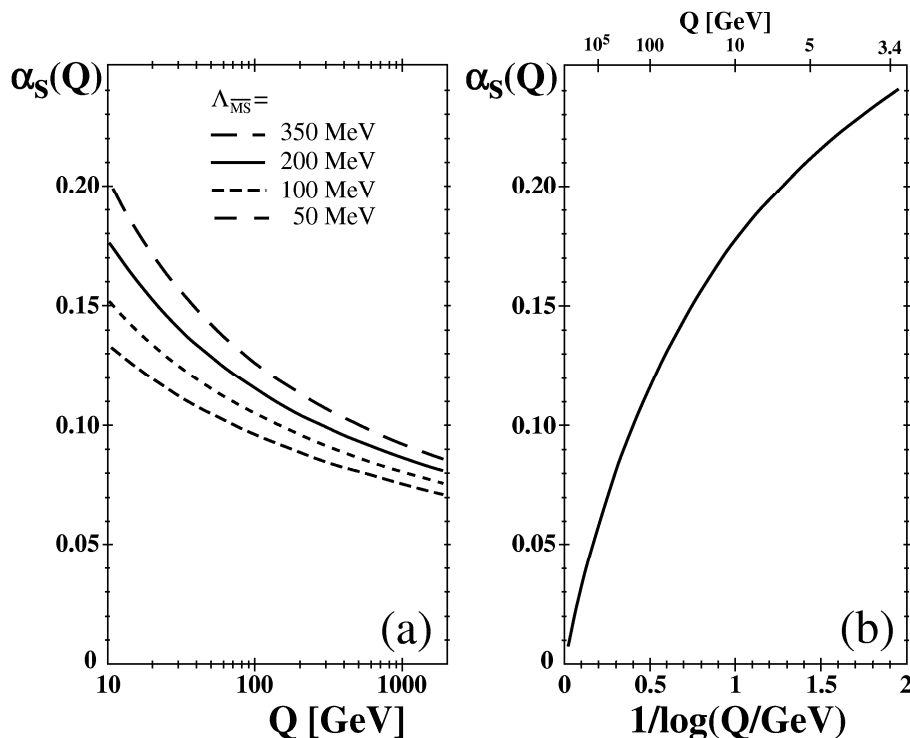


Figure 4: (a) The running of $\alpha_s(Q)$, according to equation 7, in 4-loop approximation, for different values of $\Lambda_{\overline{\text{MS}}}$; (b) same as full line in (a), but as function of $1/\log(Q/\text{GeV})$ to demonstrate asymptotic freedom, i.e. $\alpha_s(Q^2) \rightarrow 0$ for $Q \rightarrow \infty$.

3.4 The running coupling

In complete 4-loop approximation and using the Λ -parametrization, the running coupling is thus given [36] by

$$\alpha_s(Q^2) = \frac{1}{\beta_0 L} - \frac{1}{\beta_0^3 L^2} \beta_1 \ln L$$

⁴Strictly speaking, *physical observables* \mathcal{R} rather than α_s must be continuous, which may lead to small discontinuities in $\alpha_s(Q^2)$ at quark thresholds in finite order perturbation theory; see section 3.7.

$$\begin{aligned}
& + \frac{1}{\beta_0^3 L^3} \left(\frac{\beta_1^2}{\beta_0^2} (\ln^2 L - \ln L - 1) + \frac{\beta_2}{\beta_0} \right) \\
& + \frac{1}{\beta_0^4 L^4} \left(\frac{\beta_1^3}{\beta_0^3} \left(-\ln^3 L + \frac{5}{2} \ln^2 L + 2 \ln L - \frac{1}{2} \right) - 3 \frac{\beta_1 \beta_2}{\beta_0^2} \ln L + \frac{\beta_3}{2 \beta_0} \right)
\end{aligned} \tag{7}$$

where $L = Q^2/\Lambda_{\overline{MS}}^2$. The first line of equation 7 includes the 1- and the 2-loop coefficients, the second line is the 3-loop and the third line is the 4-loop correction, respectively.

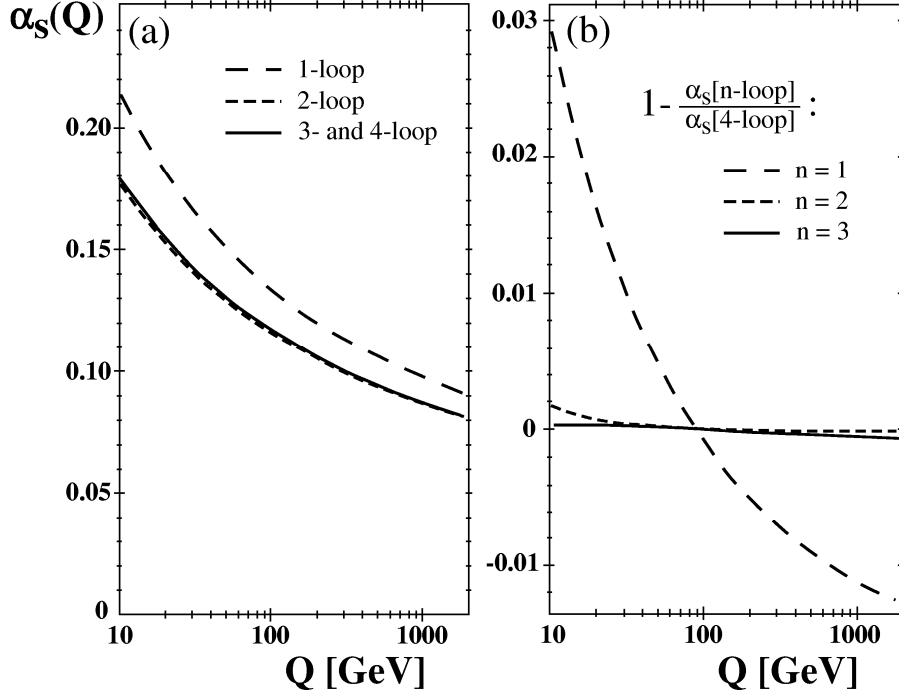


Figure 5: (a) The running of $\alpha_s(Q)$, according to equation 7, in 1-, 2- and 3-loop approximation, for $N_f = 5$ and the same value of $\Lambda_{\overline{MS}} = 0.22$ GeV. The 4-loop prediction is indistinguishable from the 3-loop curve. (b) Fractional difference between the 4-loop and the 1-, 2- and 3-loop presentations of $\alpha_s(Q)$, for $N_f = 5$ and $\Lambda_{\overline{MS}}$ chosen such that, in each order, $\alpha_s(M_{Z^0}) = 0.119$.

The functional form of $\alpha_s(Q)$, for 4 different values of $\Lambda_{\overline{MS}}$ between 50 MeV and 350 MeV, is displayed in figure 4(a). The slope and dependence on the actual value of $\Lambda_{\overline{MS}}$ is especially pronounced at small Q^2 , while at large Q^2 both the energy dependence and the dependence of $\Lambda_{\overline{MS}}$ becomes increasingly feeble. Nevertheless, α_s decreases with increasing energy scale and tends to zero at asymptotically high Q^2 . This is demonstrated in figure 4(b), where $\alpha_s(Q^2)$ is plotted as a function of $1/\log Q$.

Any experimental proof of asymptotic freedom will therefore require precise determinations of α_s , or of other observables which depend on $\alpha_s(Q^2)$, in a possibly large range of energy scales. This range should include as small as possible energies, since the relative energy dependence is largest there. To date, precise experimental data and respective QCD analyses are available in the range of $Q \approx 1$ GeV to a few hundred GeV.

3.5 Relative size of finite order approximations

The importance of higher order loop corrections and the degree of convergence of the perturbative expansion for the running α_s , see equation 7, is analysed and demonstrated in figure 5. In part (a), the

1-, the 2- and the 3-loop approximation of equation 7, each with $\Lambda = 0.220$ GeV, is shown. As can be seen, there is an almost 15% decrease of α_s when changing from 1-loop to 2-loop approximation, for the same value of Λ . The difference between the 2-loop and the 3-loop prediction is only about 1-2%, and it is less than 0.01% between the 3-loop and the 4-loop presentation which cannot be resolved in the figure.

The fractional difference in the energy dependence of α_s , $\frac{(\alpha_s^{(4-loop)} - \alpha_s^{(n-loop)})}{\alpha_s^{(4-loop)}}$, for $n = 1, 2$ and 3 , is presented in figure 5(b). Here, in contrast to figure 5(a), the values of $\Lambda_{\overline{MS}}$ were chosen such that $\alpha_s(M_{Z^0}) = 0.119$ in each order, i.e., $\Lambda_{\overline{MS}} = 93$ MeV (1-loop), $\Lambda_{\overline{MS}} = 239$ MeV (2-loop), and $\Lambda_{\overline{MS}} = 220$ MeV (3- and 4-loop). Only the 1-loop approximation shows sizeable differences of up to several per cent, in the energy and parameter range chosen, while the 2- and 3-loop approximation already reproduce the energy dependence of the best, i.e. 4-loop, prediction quite accurately.

3.6 Quark masses and thresholds

So far in this discussion, finite quark masses m_q were neglected, assuming that both the physical and the renormalization scales Q^2 and μ^2 , respectively, are larger than any other relevant energy or mass scale involved in the problem. This is, however, not entirely correct, since there are several QCD studies and α_s determinations at energy scales around the charm- and bottom-quark masses of about 1.5 and 4.7 GeV, respectively.

Finite quark masses may have two major effects on actual QCD studies: Firstly, quark masses will alter the perturbative predictions of observables \mathcal{R} . While phase space effects which are introduced by massive quarks can often be studied using hadronization models and Monte Carlo simulation techniques, explicit quark mass corrections in higher than leading perturbative order are available only for very few observables.

Secondly, any quark-mass dependence of \mathcal{R} will add another term $\mu^2 \frac{\partial m}{\partial \mu^2} \frac{\partial}{\partial m} \mathcal{R}$ to equation 1, which leads to energy-dependent, running quark masses, $m_q(Q^2)$, in a similar way as the running coupling $\alpha_s(Q^2)$ was obtained.

In addition to these effects, α_s indirectly also depends on the quark masses, through the dependence of the β coefficients on the effective number of quarks flavours, N_f , with $m_q \ll \mu$. Constructing an effective theory for, say, (N_f-1) quark flavours which must be consistent with the N_f quark flavours theory at the heavy quark threshold $\mu^{(N_f)} \sim \mathcal{O}(m_q)$, results in matching conditions for the α_s values of the (N_f-1) - and the N_f -quark flavours theories [37].

In leading and in next-to-leading order, the matching condition is $\alpha_s^{(N_f-1)} = \alpha_s^{N_f}$. In higher orders and the \overline{MS} scheme, however, nontrivial matching conditions apply [37, 38, 36]. Formally these are, if the energy evolution of α_s is performed in n^{th} order, of order $(n-1)$.

The matching scale $\mu^{(N_f)}$ can be chosen in terms of the (running) \overline{MS} mass $m_q(\mu_q)$, or of the constant, so-called pole mass M_q . For both cases, the relevant matching conditions are given in [36]. These expressions have a particularly simple form for the choice⁵ $\mu^{(N_f)} = m_q(m_q)$ or $\mu^{(N_f)} = M_q$. In this report, the latter choice will be used to perform 3-loop matching at the heavy quark pole masses, in which case the matching condition reads, with $a = \alpha_s^{(N_f)}/\pi$ and $a' = \alpha_s^{(N_f-1)}/\pi$:

$$\frac{a'}{a} = 1 + C_2 a^2 + C_3 a^3, \quad (8)$$

where $C_2 = -0.291667$ and $C_3 = -5.32389 + (N_f - 1) \cdot 0.26247$ [36].

The 4-loop prediction for the running α_s , using equation 7 with $\Lambda_{\overline{MS}}^{(N_f=5)} = 220$ MeV and 3-loop matching at the charm- and bottom-quark pole masses, $\mu_c^{(N_f=4)} = M_c = 1.5$ GeV and $\mu_b^{(N_f=5)} = M_b =$

⁵The results of reference [36] are also valid for other relations between $\mu^{(N_f)}$ and m_q or M_q , as e.g. $\mu^{(N_f)} = 2M_q$. For 3-loop matching, however, practical differences due to the freedom of this choice are negligible.

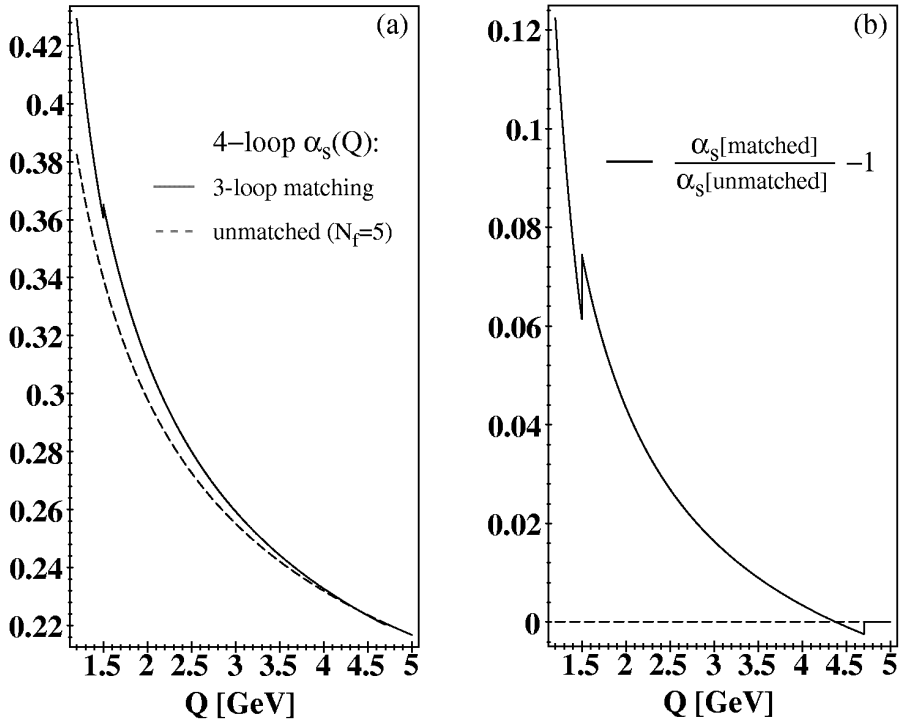


Figure 6: (a) 4-loop running of $\alpha_s(Q)$ with 3-loop quark threshold matching according to equations 7 and 8, with $\Lambda_{\overline{MS}}^{(N_f=5)} = 220$ MeV and charm- and bottom-quark thresholds at the pole masses, $\mu_c^{(N_f=4)} \equiv M_c = 1.5$ GeV and $\mu_b^{(N_f=5)} \equiv M_b = 4.7$ GeV (full line), compared with the unmatched 4-loop result (dashed line). (b) The fractional difference between the two curves in (a).

4.7 GeV, is illustrated in figure 6a (full line). Small discontinuities at the quark thresholds can be seen, such that $\alpha_s^{(N_f-1)} < \alpha_s^{(N_f)}$ by about 2 per mille at the bottom- and about 1 per cent at the charm-quark threshold. The corresponding values of $\Lambda_{\overline{MS}}$ are $\Lambda_{\overline{MS}}^{(N_f=4)} = 305$ MeV and $\Lambda_{\overline{MS}}^{(N_f=3)} = 346$ MeV. Comparison with the 4-loop prediction, without applying threshold matching and for $\Lambda_{\overline{MS}}^{(N_f=5)} = 220$ MeV and $N_f = 5$ throughout (dashed line) demonstrates that, in addition to the discontinuities, the matched calculation shows a steeper rise towards smaller energies because of the larger values of $\Lambda_{\overline{MS}}^{(N_f=4)}$ and $\Lambda_{\overline{MS}}^{(N_f=3)}$.

The size of discontinuities and the changes of slopes are demonstrated in figure 6b, where the fractional difference between the two curves from figure 6a, i.e. between the matched and the unmatched calculation, is presented. Note that the step function of α_s is not an effect which can be measured; the steps are artifacts of the truncated perturbation theory and the requirement that predictions for observables at energy scales around the matching point must be consistent and independent of the two possible choices of (neighbouring) values of N_f .

3.7 Perturbative predictions of physical quantities

In practice, α_s is not an ‘observable’ by itself. Values of $\alpha_s(\mu^2)$ are determined from measurements of observables \mathcal{R} for which QCD predictions exist. In perturbative QCD, these are usually given by a power series in $\alpha_s(\mu^2)$, like

$$\mathcal{R}(Q^2) = P_l \sum_n R_n \alpha_s^n$$

$$= P_l \left(R_0 + R_1 \alpha_s(\mu^2) + R_2(Q^2/\mu^2) \alpha_s^2(\mu^2) + \dots \right), \quad (9)$$

where R_n are the n_{th} order coefficients of the perturbation series and $P_l R_0$ denotes the lowest-order value of \mathcal{R} .

For processes which involve gluons already in lowest order perturbation theory, P_l itself may include (powers of) α_s . For instance, this happens in case of the hadronic decay width of heavy Quarkonia, $\Gamma(\Upsilon \rightarrow ggg \rightarrow \text{hadrons})$ for which $P_l \propto \alpha_s^3$. If no gluons are involved in lowest order, as e.g. in $e^+e^- \rightarrow q\bar{q} \rightarrow \text{hadrons}$ or in deep inelastic scattering processes, $P_l R_0$ is a constant and the usual choice of normalisation is $P_l \equiv 1$. R_0 is called the *lowest order* coefficient and R_1 is the *leading order* (LO) coefficient. Following this naming convention, R_2 is the *next-to-leading order* (NLO) and R_3 is the *next-to-next-to-leading order* (NNLO) coefficient.

QCD calculations in NLO perturbation theory are available for many observables \mathcal{R} in high energy particle reactions like hadronic event shapes, jet production rates, scaling violations of structure functions. Calculations including the complete NNLO are available for some totally inclusive quantities, like the total hadronic cross section in $e^+e^- \rightarrow \text{hadrons}$, moments and sum rules of structure functions in deep inelastic scattering processes, the hadronic decay widths of the Z^0 boson, of the τ lepton and of heavy quarkonia like the Υ and the J/Ψ . The complicated nature of QCD, due to the process of gluon self-coupling and the resulting large number of Feynman diagrams in higher orders of perturbation theory, so far limited the number of QCD calculations in complete NNLO.

Another approach to calculating higher order corrections is based on the resummation of logarithms which arise from soft and collinear singularities in gluon emission [39]. Application of resummation techniques and appropriate matching with fixed-order calculations are further detailed e.g. in [32].

3.8 Renormalization scale dependence.

The principal independence of a physical observable \mathcal{R} from the choice of the renormalization scale μ was expressed in equation 1. Replacing α_s by $\alpha_s(\mu^2)$, using equation 2, and inserting the perturbative expansion of \mathcal{R} (equation 9) into equation 1 results, for processes with constant P_l , in

$$\begin{aligned} 0 = \mu^2 \frac{\partial R_0}{\partial \mu^2} + \alpha_s(\mu^2) \mu^2 \frac{\partial R_1}{\partial \mu^2} &+ \alpha_s^2(\mu^2) \left[\mu^2 \frac{\partial R_2}{\partial \mu^2} - R_1 \beta_0 \right] \\ &+ \alpha_s^3(\mu^2) \left[\mu^2 \frac{\partial R_3}{\partial \mu^2} - [R_1 \beta_1 + 2R_2 \beta_0] \right] \\ &+ \mathcal{O}(\alpha_s^4). \end{aligned} \quad (10)$$

Solving this relation requires that the coefficients of $\alpha_s^n(\mu^2)$ vanish for each order n . With an appropriate choice of integration limits one thus obtains

$$\begin{aligned} R_0 &= \text{const.}, \\ R_1 &= \text{const.}, \\ R_2 \left(\frac{Q^2}{\mu^2} \right) &= R_2(1) - \beta_0 R_1 \ln \frac{Q^2}{\mu^2}, \\ R_3 \left(\frac{Q^2}{\mu^2} \right) &= R_3(1) - [2R_2(1)\beta_0 + R_1\beta_1] \ln \frac{Q^2}{\mu^2} + R_1\beta_0^2 \ln^2 \frac{Q^2}{\mu^2} \end{aligned} \quad (11)$$

as a solution of equation 10.

Invariance of the complete perturbation series against the choice of the renormalization scale μ^2 therefore implies that the coefficients R_n , except R_0 and R_1 , explicitly depend on μ^2 . In infinite order, the renormalization scale dependence of α_s and of the coefficients R_n cancel; in any finite (truncated)

order, however, the cancellation is not perfect, such that all realistic perturbative QCD predictions include an explicit dependence on the choice of the renormalization scale.

This dependence is most pronounced in leading order QCD because R_1 does not explicitly depend on μ and thus, there is no cancellation of the (logarithmic) scale dependence of $\alpha_s(\mu^2)$ at all. Only in next-to-leading and higher orders, the scale dependence of the coefficients R_n , for $n \geq 2$, partly cancels that of $\alpha_s(\mu^2)$. In general, the degree of cancellation improves with the inclusion of higher orders in the perturbation series of \mathcal{R} .

Renormalization scale dependence is often used to test and specify uncertainties of theoretical calculations and predictions of physical observables. In most studies, the central value of $\alpha_s(\mu^2)$ is determined or taken for μ equalling the typical energy of the underlying scattering reaction, like e.g. $\mu^2 = E_{cm}^2$ in e^+e^- annihilation, and changes of the result when varying this definition of μ within “reasonable ranges” are taken as systematic uncertainties.

There are several proposals of how to optimize or fix the renormalisation scale, see e.g. [40, 41, 42, 43] Unfortunately, there is no common agreement of how to optimize the choice of scales or how to define the size of the corresponding uncertainties. This unfortunate situation should be kept in mind when comparing and summarising results from different analyses.

For more details and examples on renormalisation scale dependences see e.g. [32].

3.9 Nonperturbative QCD methods

At large distances or low momentum transfers, α_s becomes large and application of perturbation theory becomes inappropriate. Nonperturbative methods have therefore been developed to describe strong interaction processes at low energy scales of typically $Q^2 < 1 \text{ GeV}^2$, such as the fragmentation of quarks and gluons into hadrons (“hadronisation”) and the absolute masses and mass splittings of mesons.

Hadronisation models are used in Monte Carlo approaches to describe the transition of quarks and gluons into hadrons. They are based on QCD-inspired mechanisms like the “string fragmentation” [44, 45] or “cluster fragmentation” [46]. Those models usually contain a number of free parameters which must be adjusted in order to reproduce experimental data well. They are indispensable tools not only for detailed QCD studies of high energy collision reactions, but are also important to assess the resolution and acceptance of experimental setups.

Power corrections are an analytic approach to approximate nonperturbative hadronisation effects by means of perturbative methods, introducing a universal, non-perturbative parameter

$$\alpha_0(\mu_I) = \frac{1}{\mu_I} \int_0^{\mu_I} dk \alpha_s(k)$$

to parametrize the unknown behaviour of $\alpha_s(Q)$ below a certain infrared matching scale μ_I [47]. Power corrections are regarded as an alternative approach to describe hadronisation effects on event shape distributions, instead of using phenomenological hadronisation models.

Lattice Gauge Theory is one of the most developed nonperturbative methods (see e.g. [48, 33]) and is used to calculate, for instance, hadron masses, mass splittings and QCD matrix elements. In Lattice QCD, field operators are applied on a discrete, 4-dimensional Euclidean space-time of hypercubes with side length a .

4 Tests of Asymptotic freedom in e^+e^- annihilations

While historical and early developments of QCD were mainly inspired by the results from deep inelastic lepton-nucleon scattering experiments, hadronic final state of e^+e^- annihilations developed into a prime-tool for precision tests of QCD, due to the availability of higher effective energies and the point-like

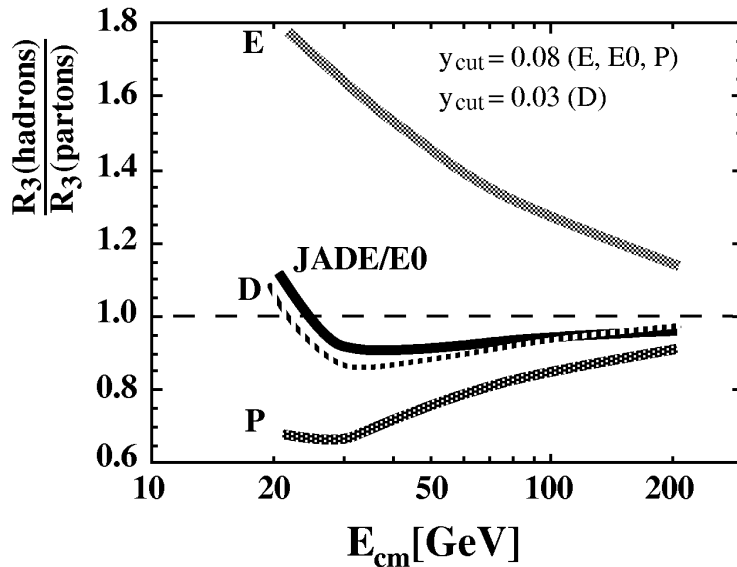


Figure 7: Energy dependence of hadronisation corrections to 3-jet event production rates, defined using various jet reconstruction schemes.

and simple nature of the primary particle reaction. Studies of hadron jets and determinations of α_s , in a wide range of centre of mass energies and with increasing experimental and theoretical precision, led to many signatures of asymptotic freedom and, equivalently important, to the evidence for colour charged gluons and the SU(3) gauge structure of QCD.

4.1 Jet production rates

The study of multijet event production rates in e^+e^- hadronic final states gave direct evidence for the energy dependence of α_s and for asymptotic freedom, before summaries of explicit measurements of α_s were able to provide a convincing case (c.f. figure 3). The basic idea was rather simple and straight-forward. It was based on a definition of resolvable jets of hadrons which could be applied both in perturbative QCD calculations and on measured hadronic final states:

Within the JADE jet algorithm [25], the scaled pair mass of two resolvable jets i and j , $y_{ij} = M_{ij}^2/E_{vis}^2$, is required to exceed a threshold value y_{cut} , where E_{vis} is the sum of the measured energies of all particles of a hadronic final state - or, in theoretical calculations, of all quarks and gluons. In a recursive process, the pair of particles or clusters of particles n and m with the smallest value of y_{nm} is replaced by (or “recombined” into) a single jet or cluster k with four-momentum $p_k = p_n + p_m$, as long as $y_{nm} < y_{cut}$. The procedure is repeated until all pair masses y_{ij} are larger than the jet resolution parameter y_{cut} , and the remaining clusters of particles are called jets.

Several jet recombination schemes and definitions of M_{ij} exist [49]; the original JADE scheme with $M_{ij}^2 = 2 \cdot E_i \cdot E_j \cdot (1 - \cos \theta_{ij})$, where E_i and E_j are the energies of the particles and θ_{ij} is the angle between them, and the “Durham” scheme [50] with $M_{ij}^2 = 2 \cdot \min(E_i^2, E_j^2) \cdot (1 - \cos \theta_{ij})$, were most widely used at LEP, due to their superior features like small sensitivity to hadronisation and particle mass effects [49].

The virtues of the JADE jet definition were especially suited for an early observation of the energy dependence of α_s , without the need to determine α_s and therefore avoiding the large systematic and - at that time - theoretical uncertainties:

- The relative production rate R_3 of 3-jet hadronic final states follows a particular simple theoretical

expression:

$$R_3 = \frac{\sigma(e^+e^- \rightarrow 3\text{-jets})}{\sigma(e^+e^- \rightarrow \text{hadrons})} = C_1(y_{\text{cut}}) \alpha_s(\mu^2) + C_2(y_{\text{cut}}, \mu^2) \alpha_s^2(\mu^2),$$

in NLO perturbation theory. In leading order, R_3 is thus directly proportional to α_s , and any energy dependence of R_3 observed in the data must be due to the energy dependence of α_s - if there are no other energy dependent effects. The coefficients C_1 and C_2 are energy independent. They can be reliably calculated and predicted by QCD, whereby the renormalisation scale dependence of C_2 is only a small disturbance.

- Model studies showed that hadronisation corrections to R_3 are small and, in a suitable range of centre of mass energies, almost constant, see figure 7 [26].
- The JADE jet algorithm is particularly easy to apply to measured hadronic final states, and corrections due to limited detector resolution and acceptance are small and manageable.

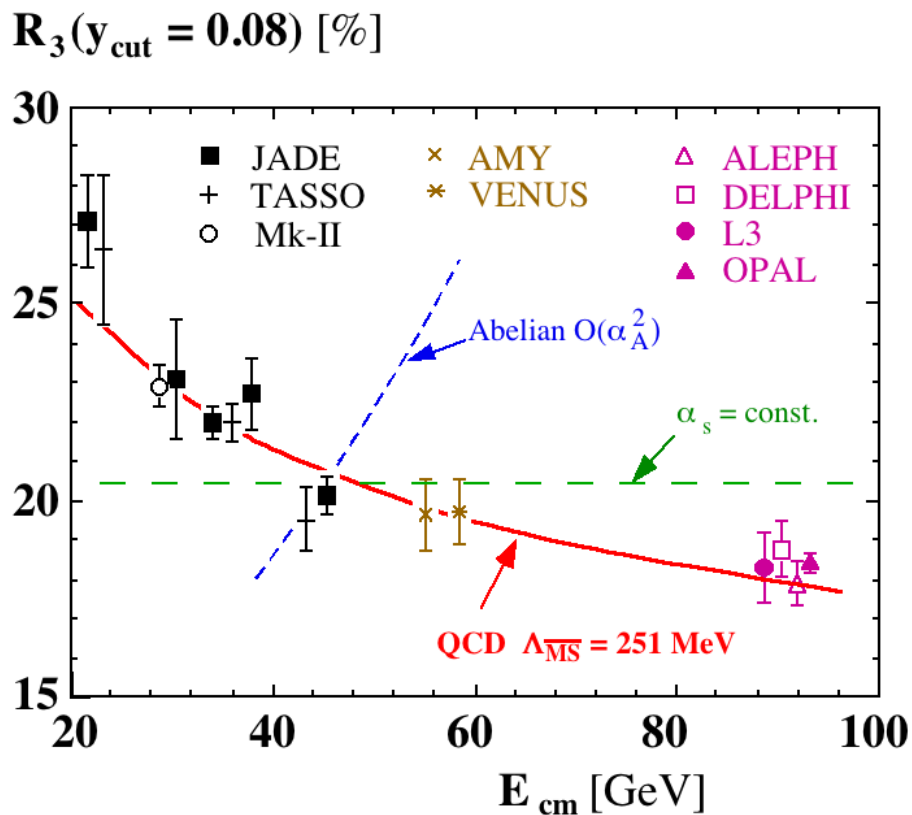


Figure 8: Energy dependence of 3-jet event production rates, measured using the JADE jet finder at a scaled jet energy resolution $y_{\text{cut}} = 0.008$. The errors are experimental. The data are not corrected for hadronisation effects. They are compared to theoretical expectations of QCD, of an abelian vector gluon model, and to the hypothesis of a constant coupling strength.

The first experimental study of the energy dependence of 3-jet event production rates, at c.m. energies between 22 and 46 GeV, analysed for constant jet resolution y_{cut} at the e^+e^- collider PETRA, gave first evidence for the energy dependence of α_s already in 1988 [26]. These data are shown in figure 8, together with more results from experiments at the PEP, TRISTAN [51] and finally, at the LEP collider [52]. The measured 3-jet rates significantly decrease with increasing centre of mass energy, in excellent agreement with the decrease predicted by QCD. The hypothesis of an energy independent

coupling, and especially the prediction of an alternative, QED-like abelian vector gluon model, where gluons carry no colour charge, are in apparent contradiction with the data [52].

In order to further demonstrate asymptotic freedom with these data, they are - combined at suitable mean energies - plotted against $1/\ln E_{cm}$, as shown in figure 9. For infinite energies, $E_{cm} \rightarrow \infty$, α_s and thus R_3 are expected to vanish to zero, which is in very good agreement with the data.

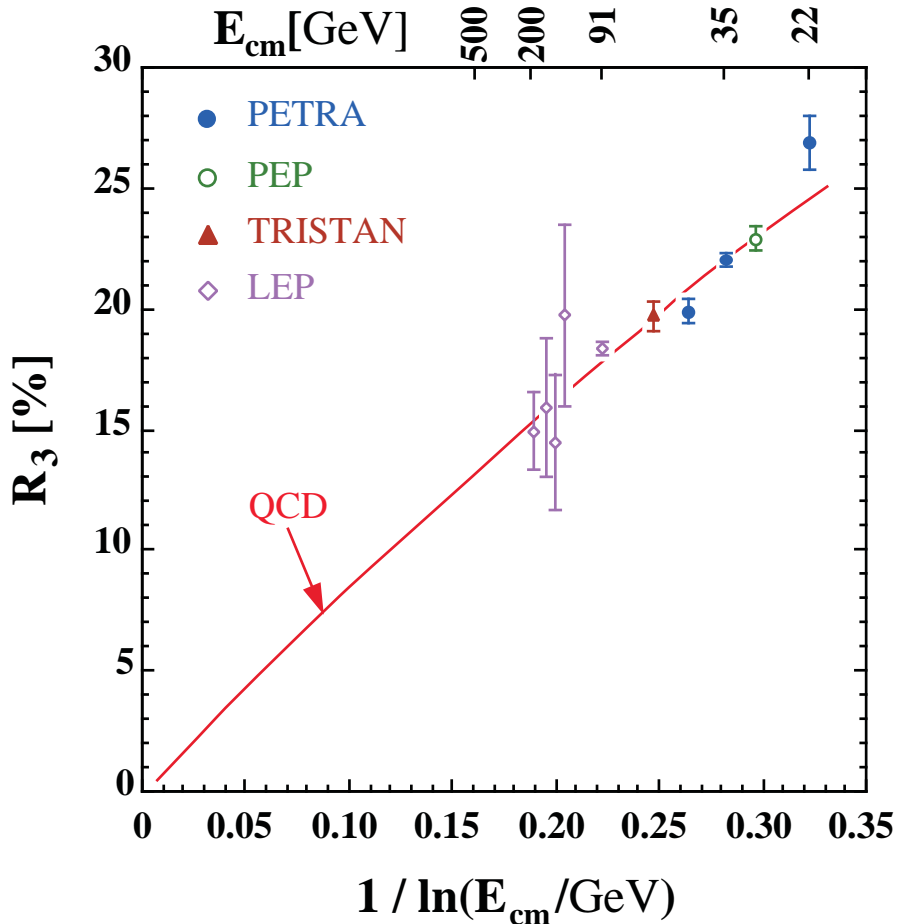


Figure 9: 3-jet event production rates as shown in Fig. 8, however as a function of $1/\ln E_{cm}$, to demonstrate that $R_3 \propto \alpha_s \rightarrow 0$ at asymptotic (i.e. infinite) energies.

4.2 Evidence for the gluon self coupling

The gluon self-coupling, as a direct consequence of gluons carrying colour charge by themselves, is essential for the prediction of asymptotic freedom. A rather direct method to detect effects of gluon-selfcoupling was accomplished at the LEP collider, by analysing distributions which are sensitive to the spin structure of hadronic 4-jet final states [27]. For instance, the so-called Bengtson-Zerwas angle, χ_{BZ} [53], measuring the angle between the planes defined by the two highest and the two lowest energy jets, is rather sensitive to the difference of a gluon-jet splitting into two gluons, which in QCD is the dominant source of 4-jet final states, and a gluon splitting to a quark-antiquark pair, which is the dominant process in an abelian vector theory where gluons carry no colour charge.

The results of an early study which showed convincing evidence for the gluon self coupling [54] after only one year of data taking, is shown in figure 10. The data clearly favour the QCD prediction and rule out the abelian vector gluon case.

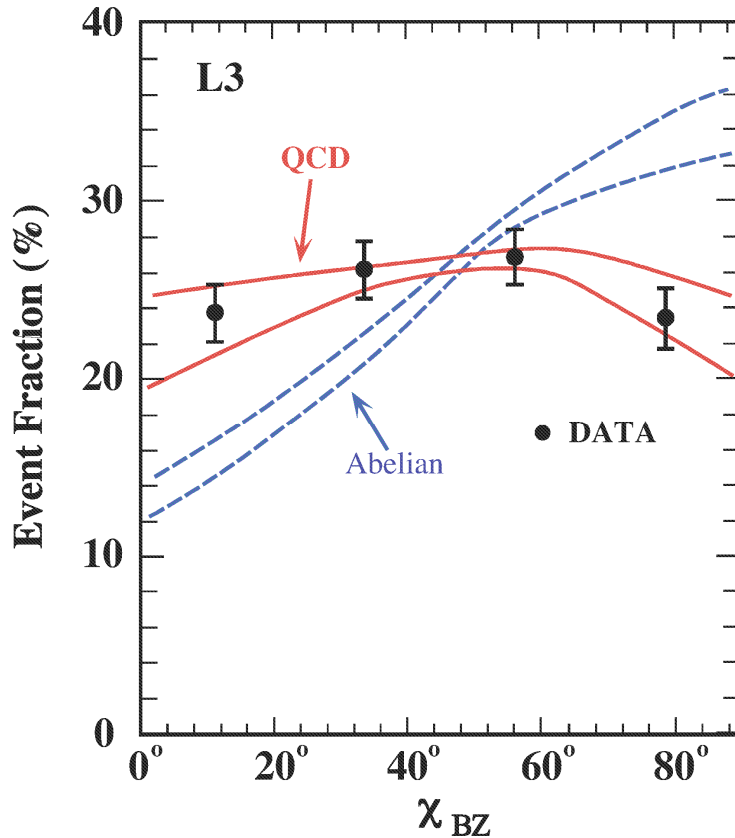


Figure 10: Distribution of the azimuthal angle between two planes spanned by the two high- and the two low-energy jets of hadronic 4-jet events measured at LEP [54], compared to the predictions of QCD and of an abelian vector gluon model where gluons carry no colour charge [27].

4.3 Determination of the QCD group constants

As already mentioned in section 3, the QCD group constants C_A , C_F and N_f , assume values of 3, 4/3 and 5 in a theory exhibiting SU(3) symmetry, with 5 quark flavours in the vacuum polarisation loops. For alternative, QED-like toy models of the strong interaction with U(1) symmetry, these values would be $C_A = 0$ and $C_F = 0.5$. Experimental determination of these two parameters can thus be regarded as one of the most intimate tests of the predictions of QCD.

At LEP, data statistics and precision allowed to actually determine experimental values for C_A , which basically is the number of colour charges, and C_F . The current state-of-the art of such studies, involving analyses of several 4-jet angular correlations or fits to hadronic event shapes, is summarised [55] in figure 11. The data, with combined values of

$$\begin{aligned} C_A &= 2.89 \pm 0.01 \text{ (stat.)} \pm 0.21 \text{ (syst.)} \\ C_F &= 1.30 \pm 0.01 \text{ (stat.)} \pm 0.09 \text{ (syst.)} \end{aligned} \quad (12)$$

are in excellent agreement with the gauge structure constants of QCD. They rule out the Abelian vector gluon model and theories exhibiting symmetries other than SU(3).

4.4 The running α_s from 4-jet event production

Since the beginning of the 1990's, advances in phenomenological calculations and predictions as well as in experimental techniques allowed to perform precision determinations of α_s , in a broad range of energies

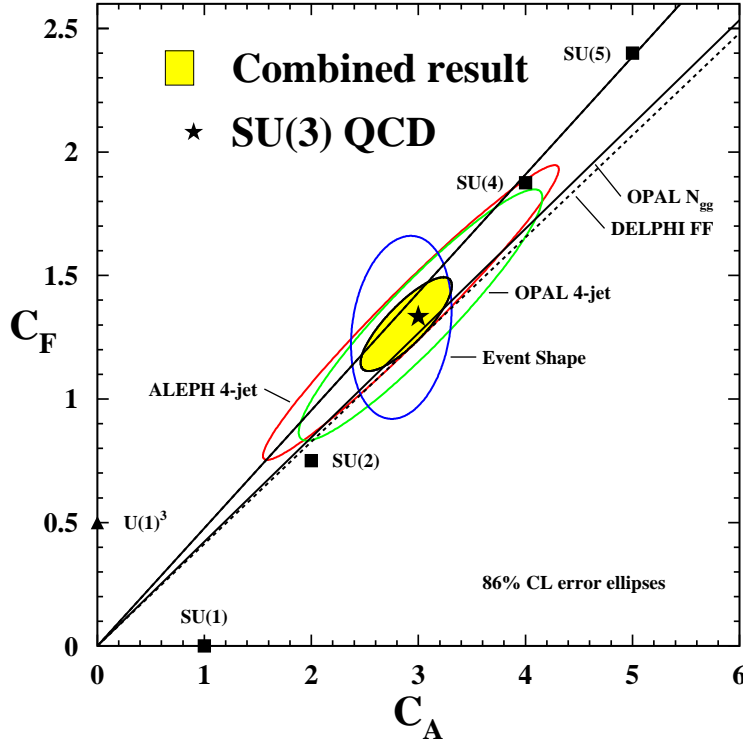


Figure 11: Measurements and combination of the QCD colour factors C_A and C_F [55].

and based on many different methods and observables. While an overall summary of α_s measurements, as presented in section 6, gives a very distinct signature for asymptotic freedom, the demonstration of the running of α_s from single experiments, minimising point-to-point systematic uncertainties, adds extra confidence in the overall conclusion.

One of the most recent developments in determining α_s in e^+e^- annihilation is the precise extraction of α_s from differential 4-jet distributions, i.e. the 4-jet production rate as a function of the jet resolution y_{cut} [56, 57, 58]. QCD predictions in NLO are available [59], which is in $\mathcal{O}(\alpha_s^3)$ perturbation theory. 4-jet final states appear only at $\mathcal{O}(\alpha_s^2)$ as their leading order, since they require at least two radiation or splitting processes off the primary quark-antiquark pair. Although “only” in NLO, the theoretical uncertainties for 4-jet observables appear to be rather small, smaller than for typical 3-jet event measures or event shapes. Since 4-jet observables are proportional to α_s^2 , they provide very sensitive measurements of α_s .

As another new development, the data of the JADE experiment, at the previous PETRA collider which was shut down in 1986, are currently re-analysed, with the experimental and theoretical experience and tools of today. This adds important new information especially at lower energies, seen from the perspective of the LEP experiments. Moreover, the JADE experiment can be regarded as the smaller brother or prototype of the OPAL detector at LEP, since both experiments were based on similar detector techniques.

A LEP-like study of α_s from 4-jet production from JADE is available [60], and is summarised in figure 12, together with the corresponding results from OPAL and the other LEP experiments. In order to appreciate the high significance for the running of α_s , one should keep in mind that only the inner (experimental) error bars need to be considered in a relative comparison of these data.

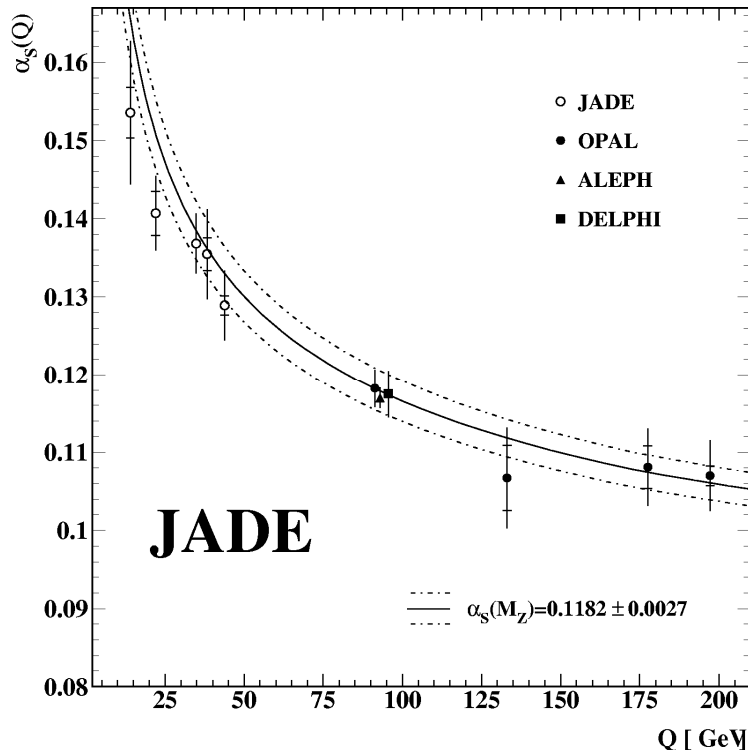


Figure 12: The values of α_s from 4-jet event production. Errors are experimental (inner marks) and the total errors [60, 56, 57, 58]. The lines indicate the QCD prediction for the running of α_s with $\alpha_s(M_{Z^0}) = 0.1182 \pm 0.0027$ [69].

5 QCD tests in deep inelastic lepton-nucleon scattering

As outlined in section 2 and 3, the observation of approximate scaling of nuclear structure functions, and thereafter, with higher precision and extended ranges of x and Q^2 , of (logarithmic) scaling violations, originally boosted the development of the quark-parton model and of QCD. The limited range of fixed-target lepton-nucleon scattering experiments in x and Q^2 , however, prevented significant and unambiguous tests of QCD scaling violations and the running of α_s , see e.g. [24].

This picture changed dramatically when the HERA electron-proton and positron-proton collider started operation in 1991, with lepton beam energies of 30 GeV and protons of 920 GeV. HERA extended the range in Q^2 by more than 2 orders of magnitude towards higher values, and the range in x by more than 3 orders of magnitude towards smaller values. With these parameters, precise tests of scaling violations of structure functions, but also precise determinations of the running α_s from jet production were achieved. While these two topics will be reviewed in the following subsections, a summary of significant α_s determination in deep inelastic scattering will be included in section 6, see also [32, 81, 69].

5.1 Basic introduction to structure functions

Cross sections of physical processes in lepton-nucleon scattering and in hadron-hadron collisions depend on the quark- and gluon-densities in the nucleon. Assuming factorisation between short-distance, hard scattering processes which can be calculated using QCD perturbation theory, and low-energy or long-range effects which are not accessible by perturbative methods, such cross sections are parametrized by a set of structure functions F_i ($i = 1, 2, 3$). The transition between the long- and the short-range

regimes is defined by an arbitrary factorization scale μ_f , which — in general — is independent from the renormalization scale μ , but has similar features as the latter: the higher order coefficients of the perturbative QCD series for physical cross sections depend on μ_f in such a way that the cross section to all orders must be independent of μ_f , i.e. $\mu_f \partial \sigma / \partial \mu_f = 0$. To simplify application of theory to experimental measurements, the assumption $\mu_f = \mu$ is usually made, with $\mu \equiv Q$ as the standard choice of scales.

In the naive quark-parton model, i.e. neglecting gluons and QCD, and for zero proton mass, the differential cross sections for electromagnetic charged lepton (electron or muon) - proton scattering off an unpolarized proton target is written

$$\frac{d^2 \sigma^{em}}{dx dQ^2} = \frac{4\pi\alpha^2}{Q^4} \left[[1 + (1+y)^2] F_1^{em} + \frac{(1-y)}{x} (F_2^{em} - 2xF_1^{em}) \right], \quad (13)$$

where, for fixed target reactions, $x = \frac{Q^2}{2M(E-E')}$ is the nucleon momentum fraction carried by the struck parton, $y = 1 - E'/E$, Q^2 is the negative quadratic momentum transfer in the scattering process, and M , E and E' are the mass of the proton and the lepton energies before and after the scattering, respectively, in the rest frame of the proton. In the quark-parton model, these structure functions consist of combinations of the quark- and antiquark densities $q(x)$ and $\bar{q}(x)$ for both valence- (u,d) and sea-quarks (s,c).

In QCD, the gluon content of the proton as well as higher order diagrams describing photon/gluon scattering, $\gamma g \rightarrow q\bar{q}$, QCD Compton processes $\gamma q \rightarrow gq$ and gluon radiation off quarks must be taken into account. Quark- and gluon-densities, the structure functions F_i and physical cross sections become energy (Q^2) dependent. QCD thus predicts, departing from the naive quark-parton model, scaling violations in physical cross sections, which are associated with the radiation of gluons. While perturbative QCD cannot predict the functional form of parton densities and structure functions, their energy evolution is described by the so-called DGLAP equations [61, 62].

The energy dependence of structure functions are known, since the early 1980's, in NLO QCD [63]. Recently, parts of the NNLO predictions became available, see e.g. [65, 64], and should be completely known in NNLO fairly soon. Apart from terms whose energy dependence is given by perturbative QCD, structure functions contain so-called “higher twist” contributions (HT). The leading higher twist terms are proportional to $1/Q^2$; they are numerically important at low $Q^2 < \mathcal{O}(\text{few GeV}^2)$ and at very large $x \simeq 1$.

5.2 Scaling violations of structure functions

A recent summary of measurements of the proton structure function F_2 is given in figure 13 [66]. The measurements cover an impressively large parameter space in x and Q^2 . The degree of scaling violations predicted by QCD [11], namely a strong increase of F_2 with increasing Q^2 at small x , and a decrease of F_2 at $x > 0.1$, is clearly reproduced by the data. Over the whole kinematic range, the data are in very good agreement with the structure function evolution as predicted by QCD.

One of the most important results obtained from HERA was, in fact, the discovery of the strong rise of F_2 at small x , as demonstrated again in figure 14. It proves the QCD picture of an increasing part of the proton consisting of gluons, i.e. field energy, if the resolution is increased (c.f. section 2.5). Another way to demonstrate the compatibility of the observed scaling violations with the predictions of QCD is to analyse the logarithmic slopes, $\partial F_2(x, Q^2) / \partial \ln Q^2$ as a function of x , as shown in figure 15. Again, QCD provides an excellent description of the data.

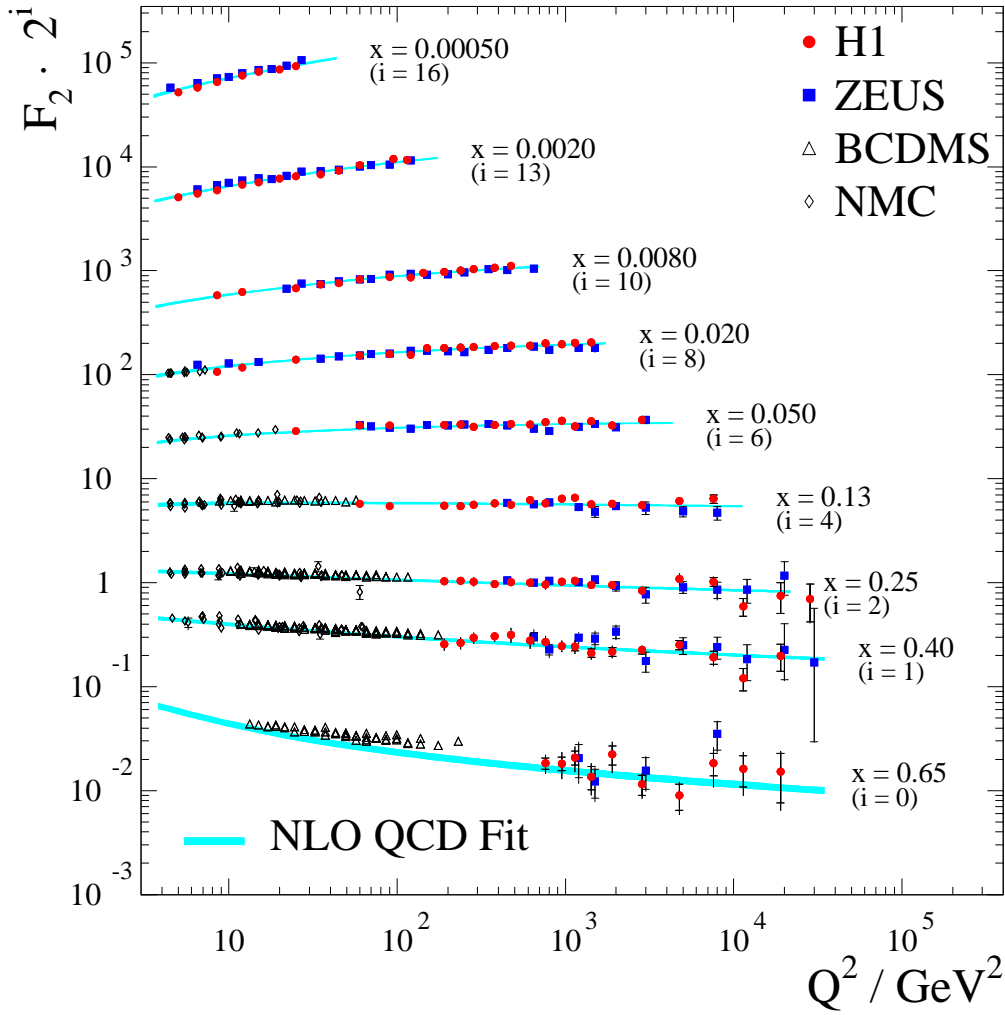


Figure 13: Summary of measurements of F_2 [66]. For better visibility, the results for different values of x were multiplied with the given factors of 2^i .

5.3 The running α_s from jet production in DIS

The increase of momentum transfer Q^2 at HERA also allowed to see and analyse the jet structure in deep inelastic scattering processes. Here, similar as in e^+e^- annihilations, production of multijet final states is predicted in QCD to NLO, and allows to determine α_s in a large range of energy scales.

Inclusive as well as differential jet production rates were studied in the energy range of $Q^2 \sim 10$ up to 10000 GeV^2 , using similar jet definitions and algorithms as in e^+e^- annihilation. In leading order α_s , $2 + 1$ jet events in deep inelastic ep scattering arise from photon-gluon fusion and from QCD Compton processes. The term ‘ $2 + 1$ jet’ denotes events where two resolved jets can be identified at large momentum transfer, in addition to the beam jet from the remnant of the incoming proton.

A recent summary of α_s determinations from the two HERA experiments H1 and ZEUS is given in figure 16 [67]. Here, the transverse jet energy E_T^{jet} was chosen as the relevant energy scale. Both experiments have determined α_s at several different values of E_T^{jet} , and the summary of all these results clearly demonstrates that α_s runs as predicted by QCD.

A combination of these results [67] will be included in the overall summary of α_s determinations, which is presented in the following section.

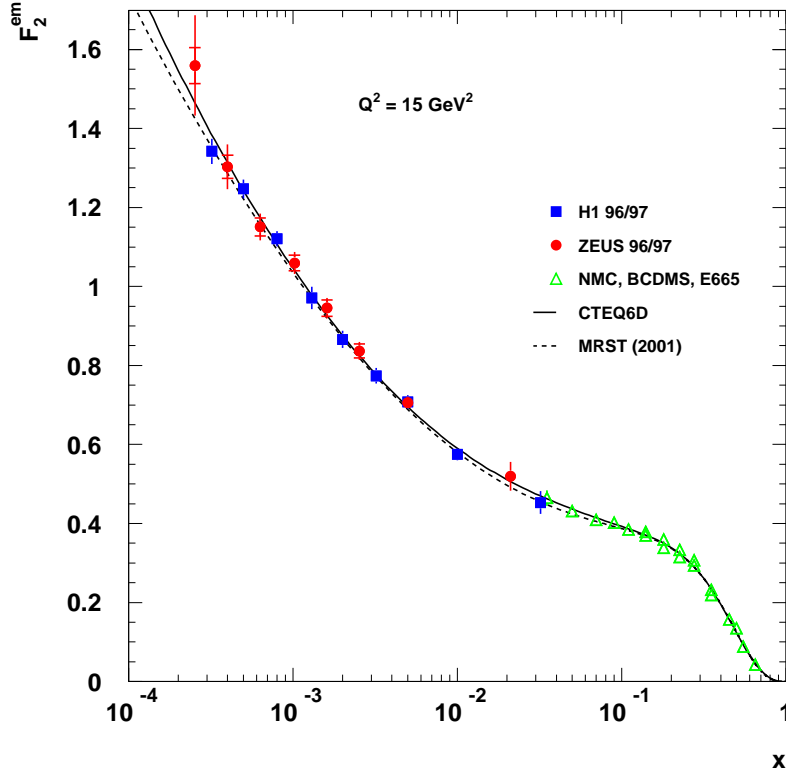


Figure 14: Proton structure function $F_2(x, Q^2)$ [66], as a function of x , demonstrating the strong rise at very small values of x .

6 Summary of α_s measurements

6.1 Previous developments and current status

By the end of the 1980's, as concluded in section 2.11 above, summaries of measurements of α_s demonstrated very good agreement with the prediction of asymptotic freedom (c.f. figure 3), but both the precision and the energy range of the results did not yet allow to claim firm evidence for the running of α_s .

This situation changed significantly with the turn-on of the LEP e^+e^- collider in 1989, with advancements in theoretical calculations and predictions, and with improved experimental methods to determine α_s . At LEP, after the first successful year of data taking, precise results emerged at high energies, i.e. at the Z^0 mass peak, $E_{cm} = M_{Z^0} = 91.2$ GeV, and also at very small energy scales of $M_\tau = 1.78$ GeV, extending the energy range and improving the overall precision by significant amounts.

This in turn quickly led to a very consistent picture: the experimental results agreed with the prediction of asymptotic freedom in the energy range from the τ to the Z^0 mass, and were compatible with a common value of $\alpha_s(M_{Z^0}) = 0.117 \pm 0.004$ [68]. The theoretical uncertainties of this average were, and still are today, a matter of discussion.

The number of precise measurements of α_s continued to grow, especially from the HERA collider, from hadron collisions at the Tevatron, and from the study of heavy quarkonia masses and decays. Through LEP-II and the Tevatron, the energy scale of α_s determinations was extended to 200 GeV

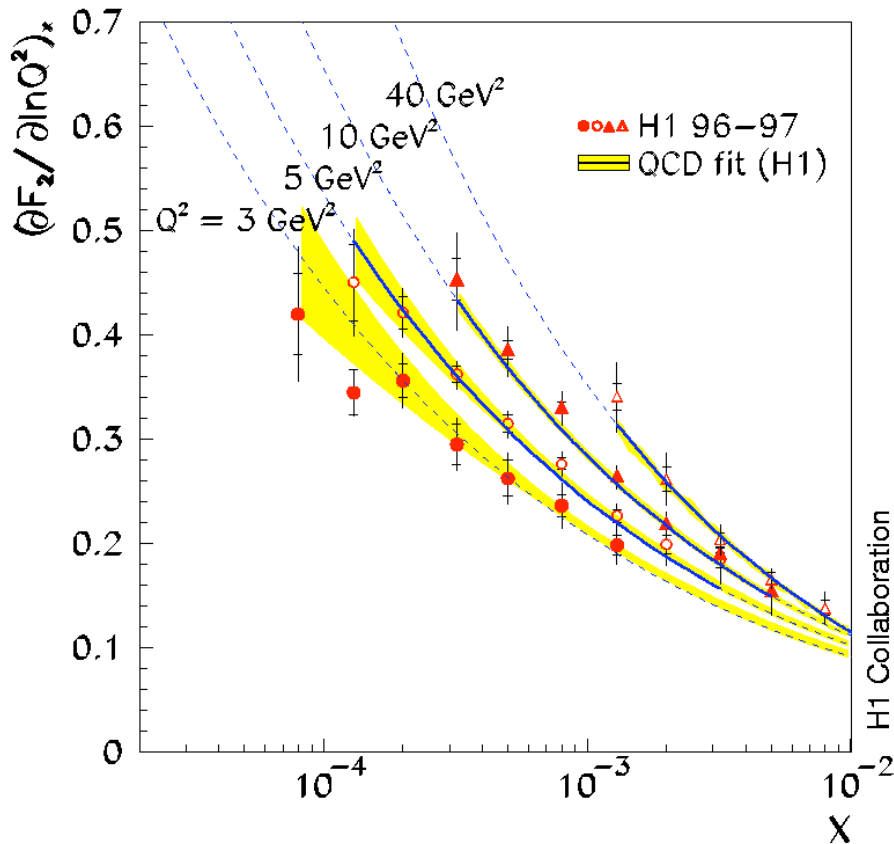


Figure 15: Logarithmic slope of $F_2(x, Q^2)$ as a function of x .

and beyond. The precision of many measurements and theoretical calculations was increased, and the number of observables and measurements which were based on complete NNLO QCD predictions grew. A comprehensive summary of the state-of-the-art of α_s determinations was given e.g. in [32] and was continuously updated in [81, 69], leading to a combined world average of $\alpha_s(M_{Z^0}) = 0.1182 \pm 0.0027$ in 2004⁶.

In the following, these previous summaries will be updated, the most recent and new results will be presented, the actual evidence for asymptotic freedom will be demonstrated and a new world average of $\alpha_s(M_{Z^0})$ will be derived.

6.2 Update: new results since 2004

Since the last summary in 2004 [69], a number of new results and updates of previous studies were presented. The most significant which will be included in the overall summary and determination of the world average of $\alpha_s(M_{Z^0})$ were:

- A re-evaluation [70] of the existing data on hadronic decays of the τ -lepton and a revision of the theoretical framework, especially in terms of narrowing the range of theoretical uncertainties, resulted in a significantly improved value of $\alpha_s(M_\tau) = 0.345 \pm 0.010$, in full NNLO QCD. The total error is thereby reduced by a factor of 3, w.r.t. previous estimates [71] - which is basically due to the inclusion of available terms in NNNLO and a rather restrictive treatment of systematic

⁶For alternative summaries of α_s , leading to almost identical values of $\alpha_s(M_{Z^0})$ with a different treatment of the overall uncertainties, see e.g. [31]

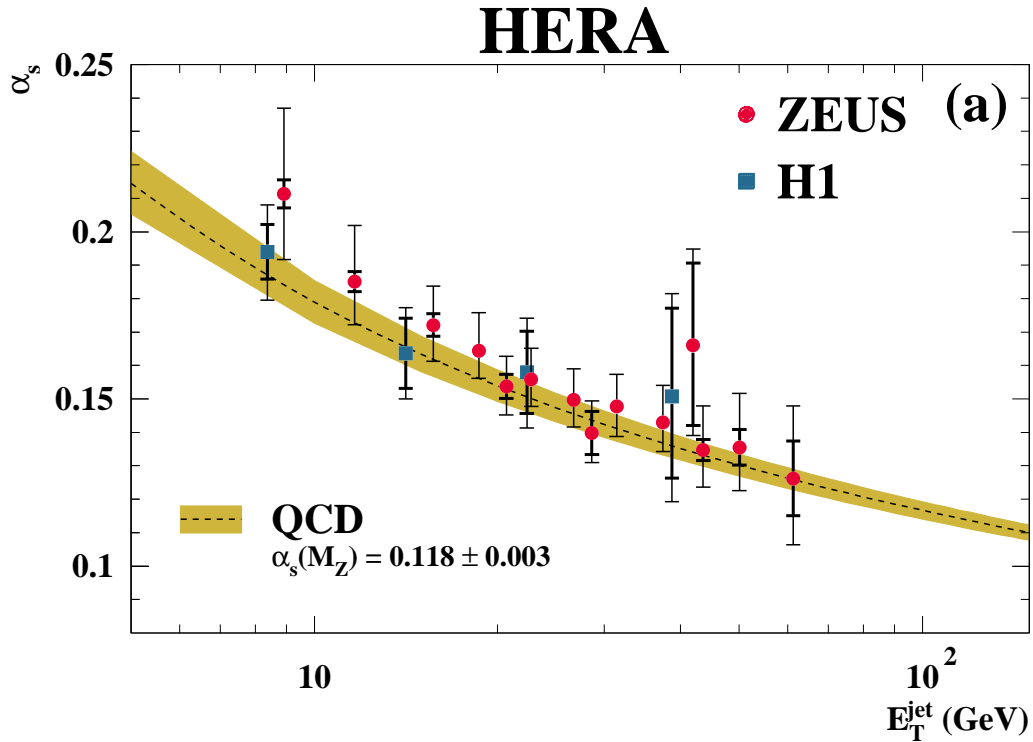


Figure 16: Results of α_s as a function of E_T^{jet} from HERA experiments H1 and ZEUS [67].

uncertainties. Although the error on this result, with a wider treatment of systematics, can well increase by a factor of 2 [72], the published value is retained for further analysis in this review.

- New analyses and a new combination of results from jet production in deep inelastic electron or positron - proton scattering at HERA [67], as shown in figure 16, provided an improved overall value of $\alpha_s(M_{Z^0}) = 0.1186 \pm 0.0051$, in NLO of perturbative QCD.
- A new study of hadron masses using predictions from lattice gauge theory, including vacuum polarisation effects from all three light quark flavours and improved third and higher order perturbative terms, resulted in a new and improved value of $\alpha_s(M_{Z^0}) = 0.1170 \pm 0.0012$ [73]. Although the methods used in this study and the small size of the claimed overall error are still under discussion [74], the published value is retained here for further discussion.
- New studies of 4-jet final states in e^+e^- annihilation at LEP [56, 57, 58, 60], see also section 4.4, and a combination of the respective α_s results give a new average of $\alpha_s(M_{Z^0}) = 0.1176 \pm 0.0022$, in $\mathcal{O}(\alpha_s^3)$ which, for 4-jet production, corresponds to NLO in perturbative QCD.

In the following overall summary of measurements of α_s , these four results will replace the respective values used in the previous summary of 2004 [69].

6.3 α_s summary

The new overall summary of α_s is given in table 1, where the new and updated results discussed in the previous section are underlined. Most of the results given in table 1 are combined from several or many individual measurements of different experiments and groups. For results obtained at fixed energy scales Q (or in narrow ranges of Q), the value of $\alpha_s(Q)$ is given, together with the extrapolation to the “standard” energy scale, $Q = M_{Z^0}$, using equation 7 in 4-loop approximation and 3-loop quark

threshold matching at the heavy quark pole masses $M_c = 1.5$ GeV and $M_b = 4.7$ GeV. Results from data in ranges of energies are only given for $Q = M_{Z^0}$. Where available, the table also contains the contributions of experimental and theoretical uncertainties to the total errors in $\alpha_s(M_{Z^0})$.

Finally, in the last two columns of table 1, the underlying theoretical calculation for each measurement and a reference to this result are given, where NLO stands for next-to-leading order, NNLO for next-next-to-leading-order of perturbation theory, “resum” stands for resummed NLO calculations which include NLO plus resummation of all leading and next-to-leading logarithms to all orders (see [39] and [32]), and “LGT” indicates lattice gauge theory.

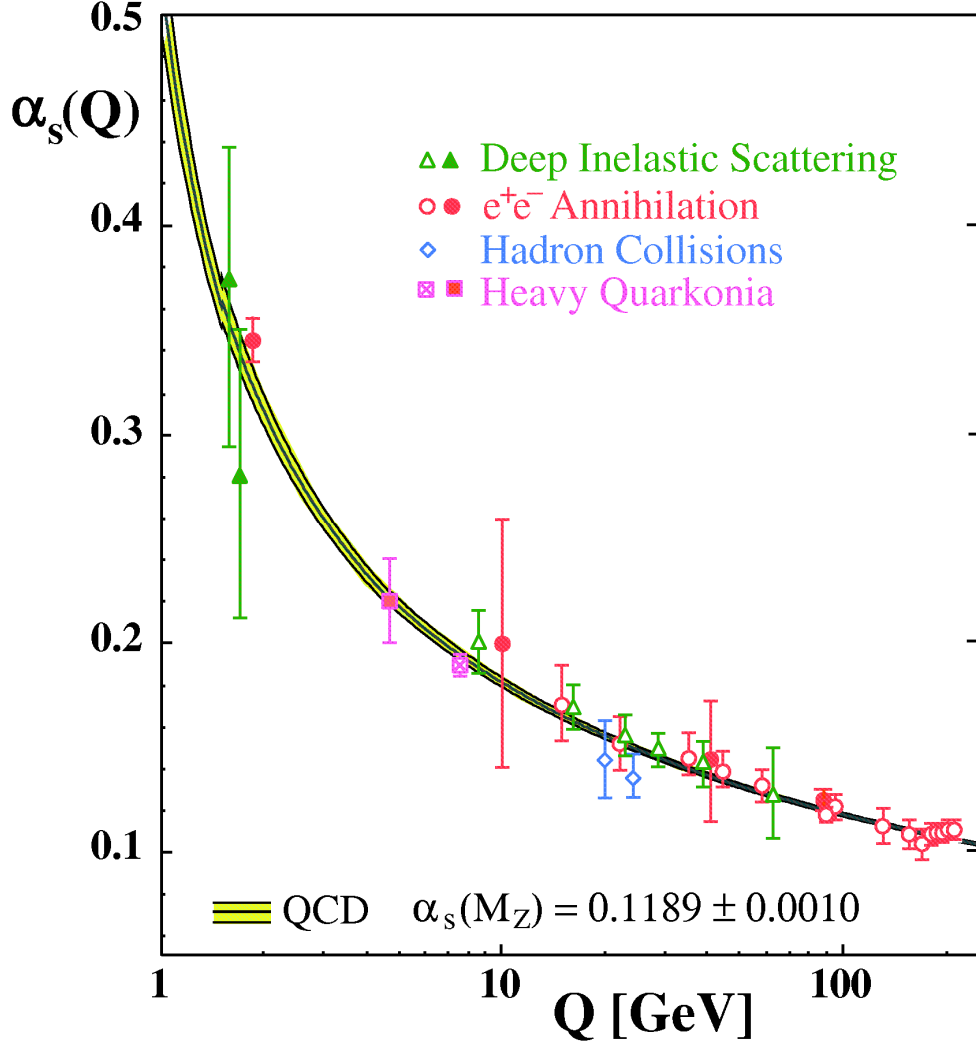


Figure 17: . Summary of measurements of $\alpha_s(Q)$ as a function of the respective energy scale Q , from table 1. Open symbols indicate (resummed) NLO, and filled symbols NNLO QCD calculations used in the respective analysis. The curves are the QCD predictions for the combined world average value of $\alpha_s(M_{Z^0})$, in 4-loop approximation and using 3-loop threshold matching at the heavy quark pole masses $M_c = 1.5$ GeV and $M_b = 4.7$ GeV.

In figure 17, all results of $\alpha_s(Q)$ given in table 1 are graphically displayed, as a function of the energy scale Q . Those results obtained in ranges of Q and given, in table 1, as $\alpha_s(M_{Z^0})$ only, are not included in this figure - with one exception: the results from jet production in deep inelastic scattering are represented in table 1 by one line, averaging over a range in Q from 6 to 100 GeV, while in figure 17 combined results for fixed values of Q as presented in [67] are displayed.

The data are compared with the QCD prediction for the running α_s , calculated for $\alpha_s(M_{Z^0}) = 0.1189 \pm 0.0010$ which - as will be discussed in the next subsection - is the new world average. The QCD curves are calculated using the 4-loop perturbative prediction, equation 7, and 3-loop quark threshold matching, see section 3.6. The data are in excellent agreement with the QCD prediction, from the smallest to the largest energy scales probed by experimental data.

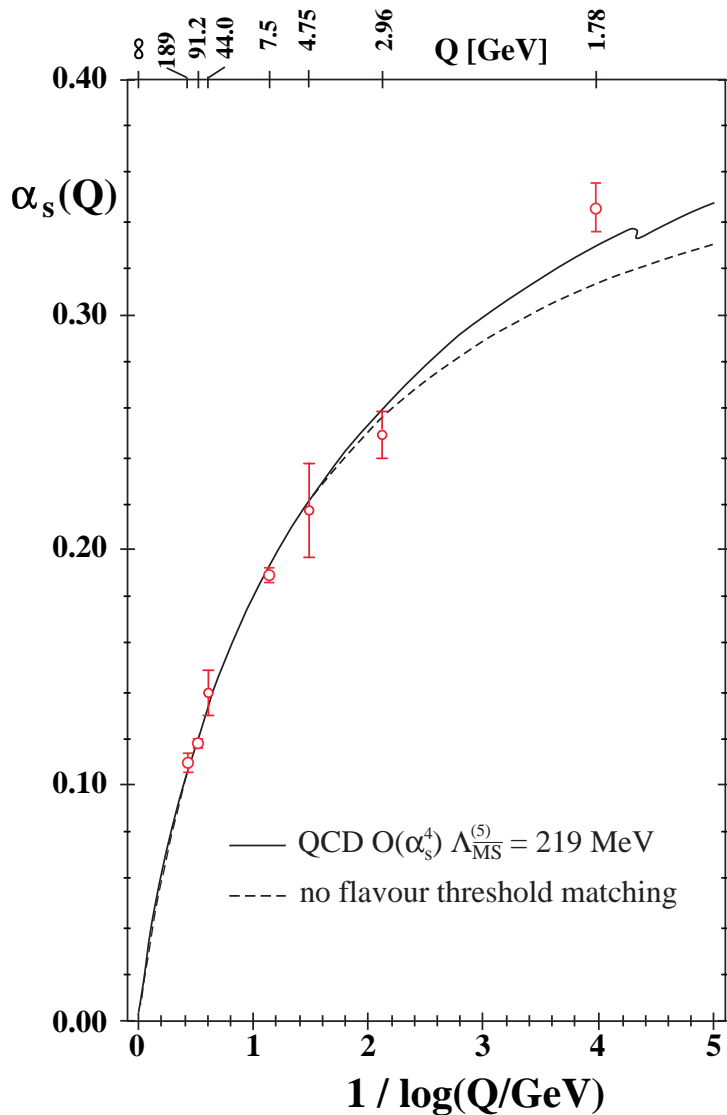


Figure 18: Some of the most significant data from figure 17, however plotted as a function of $1/\log(Q/\text{GeV})$, in order to demonstrate the significance of the data showing evidence for asymptotic freedom, i.e. the vanishing of $\alpha_s(Q)$ at asymptotically large energy scales.

In order to demonstrate the significance with which the data probe asymptotic freedom, some of the most precise α_s results are plotted⁷ in figure 18, now as a function of the inverse logarithm of Q . Also shown in this figure is the QCD prediction in 4-loop approximation including 3-loop quark threshold

⁷Only a selection of results, especially of those at high energy scales, is shown in this figure, to maintain visibility and clarity. The measurements chosen for this demonstration, from left to right, are: α_s from e^+e^- event shapes and jets at LEP-II, for ($Q = 189$ GeV), from 4-jet events at LEP ($Q = M_{Z^0} = 91.2$ GeV), from the reanalysis of e^+e^- event shapes and jets at PETRA ($Q = 44$ GeV), from hadron masses and lattice theory at $Q = 7.5$ GeV, from heavy quarkonia decays at $Q = 4.75$ GeV, and for τ -decays at $Q = 1.78$ GeV.

matching, for $\alpha_s(M_{Z^0}) = 0.1189$ (full line), and, for demonstration only, the 4-loop QCD curve omitting quark threshold matching.

The data very significantly prove the particular QCD prediction of asymptotic freedom. Apart from precisely reproducing the characteristic QCD-shape with an inverse logarithmic slope, the data point at the very lowest energies, i.e. the right-most point in figure 18, indicates that the available precision allows to conclude that quark threshold matching is necessary for QCD to consistently describe the data.

In fact, data precision is now so advanced that a rather simple QCD fit, e.g. in leading order QCD with no threshold matching, with a fit probability of less than 1%, fails to describe data⁸. Evidently, the probabilities for a hypothetical *constant* and energy *independent* α_s ⁹, or an abelian vector gluon theory which predicts an *increase* of the coupling with increasing energy scale, c.f. figure 8, have negligible probabilities to describe data. The same is true for other functional forms, like $\alpha_s \propto 1/Q$ or $\alpha_s \propto 1/Q^2$ - such functions may be adjusted such that they can describe a few data points either at low or at high values of Q , but altogether fail to describe data in the full range of energy scales from 1.78 to 200 GeV.

Therefore, it is concluded that the data, with the current precision which has substantially increased over the past few years, prove the specific QCD functional form of the running coupling α_s , and therefore of asymptotic freedom.

6.4 A new world average of $\alpha_s(M_{Z^0})$

Since all measurements of α_s , as shown in figure 17, are consistent with the running coupling as predicted by QCD, it is legitimate to evolve all values of $\alpha_s(Q)$ to a common reference energy scale, like e.g. $Q = M_{Z^0}$, using the QCD 4-loop beta-function. This was already done in the past, see e.g. [32, 69], and world average values of $\alpha_s(M_{Z^0})$ were determined.

A general difficulty in the averaging procedure is the proper and optimal treatment of errors and uncertainties. For many of the results, the dominating error is the theoretical uncertainty - which however is not uniquely defined, and is treated quite differently in most of the studies. While in a majority of analyses the theoretical uncertainty is defined through a variation of the renormalisation scale, the range of this variation is not unique. Theoretical errors, in some studies, are defined and probed in a rather restrictive and optimistic way, while in other studies they are treated in a more generous manner. Also, theoretical uncertainties are likely to be correlated between different analyses, however to an unknown degree. So the assigned errors cannot be treated like statistical and independent errors.

In previous studies [32, 81, 69], an error-weighted average and an “optimised correlation” was calculated from the error covariance matrix, assuming an overall correlation factor between the errors of the measurements included in the averaging process. This factor was adjusted such that the overall χ^2 equals unity per degree of freedom [75]. Usually the overall χ^2 was larger than unity per d.o.f., which indicated that either the individual errors were overestimated, or they were correlated. Adjusting an overall correlation factor should take care about the latter case.

The procedure, applied in a previous study to all results which are based on NNLO QCD and which have overall errors of ≤ 0.008 on $\alpha_s(M_{Z^0})$, then resulted in $\alpha_s(M_{Z^0}) = 0.1182 \pm 0.0027$ [69]. Here, the averaging shall be done using the same method, however the selection of results to be included in the final average shall be altered:

First, the restriction to results which are complete to NNLO will give a strong weight to studies at low energy scales, because most of the results obtained at high energies are in NLO, possibly including resummation, only. Second, it may be time to include the results from lattice gauge calculations, which

⁸Such a “simple” fit was previously used [32] to “fit” the β_0 coefficient of the QCD beta-function, c.f. equation 3, or - alternatively - the number of colour degrees of freedom, $C_A = N_c = 3$.

⁹In fact, there exists no theory which predicts a constant coupling.

now have reached a maturity which may be comparable to those in (NNLO) perturbation theory - and lattice gauge results are most likely *not* correlated with classical perturbation theory, thereby adding an independent input to the standard selection. Finally, in order to reach a higher degree of independence between the results included in the averaging procedure, data from different processes should be chosen, avoiding a possible bias towards any direction. In this sense, the precise determinations of α_s from 4-jet events in e^+e^- annihilation at $Q = M_z$, from event shapes and jets at $Q = 189$ GeV and from jets in deep inelastic scatterin are also chosen to be included.

Following this strategy, 10 results are henceforth selected to be included in the averaging procedure. They are summarised in table 2 and average to $\alpha_s(M_{Z^0}) = 0.1189 \pm 0.0007$, with an overall χ^2 of 9.9 for 9 degrees of freedom. Since the χ^2 is larger than unity per d.o.f., no common correlation factor needs to be assumed; in fact, in order to reach exactly 1 per d.o.f., the assigned errors of single measurements should be increased, a method which is frequently used e.g. in [31].

The fact that - in contrast to the case of previous reviews, see e.g. [32, 69] - $\chi^2/d.o.f.$ is not smaller than unity is mainly caused by two of the updates which were discussed above, namely by the new assessment of τ decays and from heavy hadron masses in lattice theory. Both have the smallest overall errors assigned - ± 0.0012 on $\alpha_s(M_{Z^0})$. Treating these as gaussian and independent errors, the two results are 2.7 standard deviations apart from each other.

The question whether one or both of these measurements has underestimated its assigned overall uncertainty cannot finally be answered. The significance of each of the 10 selected measurements can be judged from the last column of table 2, which shows the deviation of the respective average value of $\alpha_s(M_{Z^0})$ when *omitting* this particular measurement in the averaging procedure. The maximum deviation observed is $+0.0011 - 0.0013$, a value which is compatible with a total error of ± 0.0010 . The largest change in χ^2 is observed when the result from τ decays is left out - a possible hint for an underestimation of its assigned error.

Leaving out *two* of the 10 selected measurements when averaging the results gives values of $\alpha_s(M_{Z^0})$ which vary between 0.1173 and 0.1205; these two extremes again average to 0.1189 with a maximum deviation of 0.0016.

In view of these studies and variations, it is finally concluded that

$$\boxed{\alpha_s(M_{Z^0}) = 0.1189 \pm 0.0010}$$

is the new world average¹⁰ of α_s . Here, the overall error decreased by almost a factor of three as compared to the previous review [69]. This small error, however, appears to be realistic since all measurements agree well with this new average, as can be seen in figure 17: the error band is very narrow, but all the data are consistent with this result.

We have therefore reached, after 30 years of QCD, the case that not only asymptotic freedom is proven, beyond any doubts, by the data, but also that $\alpha_s(M_{Z^0})$ is now known very precisely, to better than 1% accuracy!

7 Summary and Outlook

The concept of asymptotic freedom, i.e. the QCD prediction of an inverse logarithmic decrease of the coupling strength α_s with the energy or the momentum transfer in high energy scattering reactions, was shown to be significantly and reliably verified by a number of different measurements. Historically, the first signatures for asymptotic freedom came from the observation of approximate scaling of structure functions in deep inelastic lepton-nucleon scattering experiments, and the subsequent observation of

¹⁰A small increase of the error of 0.0007 from the covariance matrix seems justified, due to the scatter of averages when leaving out one or two of the results, and due to χ^2 being slightly larger than 1 per d.o.f.

small scaling violations, in a manner as was predicted by QCD. Before specific measurements of α_s at different energy scales and processes were precise enough to prove the running of α_s , measurements of the energy dependence of jet production rates in e^+e^- annihilations provided strong evidence for the energy dependence of α_s , as predicted by QCD and by the concept of asymptotic freedom. The process of gluon self-coupling was experimentally established by studies of angular correlations within 4-jet final states, and the SU(3) gauge structure of QCD was confirmed by studies of 4-jet and event shape observables at the LEP e^+e^- collider.

Measurements of α_s , performed by single experiments over ranges of energy scales, demonstrate evidence for the running of α_s , in perfect agreement with QCD. Studies by single (or by few but similar) experiments avoid systematic uncertainties which vary from (energy) point to point, and therefore have the potential to demonstrate asymptotic freedom, however, in most cases only over a limited range of energies. Examples of such studies, as α_s from jet production in deep inelastic lepton-nucleon scattering, α_s from 4-jet event production in e^+e^- annihilation, are presented and discussed in this review.

The most significant experimental proof of asymptotic freedom today is provided by the summary and combination of all measurements of α_s , over an energy range of 1.6 GeV to more than 200 GeV, from all available processes and experiments, involving perturbative and lattice QCD calculations. The results are in excellent agreement with QCD and precisely reproduce the inverse logarithmic dependence of α_s from the energy or momentum transfer scale Q . The data prove the necessity to include higher loop diagrams in the perturbative prediction of the energy dependence of α_s , and demonstrate the need for quark flavour threshold matching of α_s , again as predicted by QCD.

Since all measurements of α_s are in excellent agreement with asymptotic freedom as predicted by QCD, the results are evolved, according to the QCD 4-loop beta-function, to a common energy scale $Q \equiv M_{Z^0}$. A set of significant and precise measurements, well balanced over all available processes, energies, experiments and theoretical methods, result in a new and improved world average value of

$$\alpha_s(M_{Z^0}) = 0.1189 \pm 0.0010 .$$

The overall uncertainty of this result is improved by almost a factor of 3, compared to the previous average presented in 2004.

This improvement will have significant implications on verifying the grand unification of forces, and in particular, on possible signatures for Supersymmetry see e.g. [94, 95]. The improvement is achieved by the inclusion of several new results and updates, like the one from τ decays, from 4-jet final states in e^+e^- annihilations at LEP, and from lattice predictions of heavy hadron masses.

The total uncertainties of these new results are in the range of 1 to 2 % only, and therefore these measurements largely dominate the determination of the world average. Although some of the quoted uncertainties may be underestimated, no significant disagreement between any of the measurements nor with the world average value of $\alpha_s(M_{Z^0})$ was found.

It is therefore concluded that the running coupling averages to the value of $\alpha_s(M_{Z^0})$ given above, with an overall uncertainty now being less than 1%.

Future prospects for precise determinations of α_s are upcoming QCD calculations, in NNLO perturbation theory, for more observables and processes, which will replace the currently used calculations in NLO or in resummed NLO, see e.g. table 1. Such calculations are in preparation by several groups, see e.g. [65, 93, 64], and the results are eagerly awaited by experimentalists. It is hoped that application of these new NNLO calculations will provide an increased number of precise α_s determinations, with overall errors of the order of 1%. This will provide the means for precise compatibility checks and for further improvements of the world average value of α_s .

Apologies and Acknowledgements.

This review is based on an almost countless number of studies and publications, comprising many hundreds of man-years of scientific and technical work on the experimental setups, on running high- and low-energy accelerators and colliders, on developing the phenomenological aspects of QCD, not all of which can be explicitly referred to in this report. I wish to thank all our colleagues who participated, in the past 30 years, in the development of QCD, and in demonstrating its experimental relevance. Apologies to those whose contributions did not receive the appropriate attention in this report. Special thanks go to Harald Fritzsch, Stefan Kluth, Peter Weisz and Peter Zerwas who were very helpful, through many fruitful discussions, with their expertise and wisdom.

References

- [1] H. Fritzsch and M. Gell-Mann, Proc. XVI Int. Conf. on High Energy Physics, Chicago-Batavia, 1972.
- [2] H. Fritzsch, M. Gell-Mann, H. Leutwyler, *Phys. Lett. B* 47 (1973) 365 .
- [3] D.J. Gross, F. Wilczek, *Phys. Rev. Lett.* 30 (1973) 1343 ; PRD 8 (1973) 3633 ;
H.D. Politzer, *Phys. Rev. Lett.* 30 (1973) 1346 .
- [4] H. Yukawa, Proc. of the Phys.-Math. Society of Japan. 17, 48 (1935)
- [5] C.M.G. Lattes, H. Muirhead, G.P.S. Occhialini, C.F. Powell, *Nature* 159 (1947) 694 .
- [6] M. Gell-Mann, *Phys. Lett.* 8 (1964) 214 ;
G. Zweig, CERN TH 401 (1964) 412 .
- [7] E.D. Bloom et al., *Phys. Rev. Lett.* 23 (1969) 930 , and *Phys. Rev. Lett.* 23 (1969) 935 .
- [8] O.W. Greenberg, *Phys. Rev. Lett.* 13 (1964) 598 .
- [9] M.Y. Han and Y. Nambu, *Phys. Rev. B* 1006 (1965) 139 .
- [10] K. Symanzik, *Comm. math. Phys.* 18 (1970) 227 .
- [11] D.J. Gross and F. Wilczek, *Phys. Rev. D* 8 (1973) 3633 ;
H. Georgi and H.D. Politzer, *Phys. Rev. D* 9 (1974) 416 .
- [12] A.J. Buras, *Rev. Mod. Phys.* 52 (1980) 199
- [13] D.W. Duke and R.G. Roberts, *Phys. Lett. B* 94 (1980) 417 .
- [14] S. Brandt et al., *Phys. Lett.* 12 (1964) 57 .
- [15] S.D. Drell, D.J. Levy, Tung-Mow Yan, *Nucl.Phys.D* 1 (1970) 1617 .
- [16] G. Hanson et al., *Phys. Rev. Lett.* 35 (1975) 1609 .
- [17] J. Ellis, M.K. Gaillard and G.G. Ross, *Nucl. Phys. B Nucl. Phys. B* 111 (1976) 253 .
- [18] R. Brandelik et al., *Phys. Lett. B* 86 (1979) 243 ;
D.P. Barber et al., *Phys. Rev. Lett.* 43 (1979) 830 ;
Ch. Berger et al., *Phys. Lett. B* 86 (1979) 418 ;
W. Bartel et al., *Phys. Lett. B* 91 (1980) 142 .
- [19] R. Brandelik et al., *Phys. Lett. B* 97 (1980) 453 ;
Ch. Berger et al., *Phys. Lett. B* 97 (1980) 459 ;
H.J. Behrend et al., *Phys. Lett. B* 110 (1982) 329 .
- [20] P. Hoyer et al., *Nucl. Phys. B* 161 (1979) 349 .
- [21] A. Ali et al., *Phys. Lett. B* 93 (1980) 155 .
- [22] JADE Collaboration, W. Bartel et al., *Phys. Lett. B* 101 (1981) 129 ; *Z. Phys. C* 21 (1983) 37 .

- [23] B. Andersson, G. Gustafson and T. Sjöstrand, *Z. Phys. C* 6 (1980) 235 ; and *Nucl. Phys. B* 197 (1982) 45 .
- [24] G. Altarelli, *Ann.Rev.Nucl.Part.Sci.* 39 (1989) 357 .
- [25] W. Bartel et al., *Z. Phys. C* 33 (1986) 23 .
- [26] S. Bethke et al., *Phys. Lett. B* 213 (1988) 235 .
- [27] S. Bethke, A. Ricker and P.M. Zerwas, *Z. Phys. C* 49 (1991) 59 .
- [28] R.K. Ellis, W.J. Stirling and B.R. Webber, *QCD and Collider Physics*, Cambridge University Press, 1996.
- [29] J.C. Collins, *Renormalization*, Cambridge University Press, 1984.
- [30] T. Muta, *World Sci. Lect. Notes Phys.* 57 (1998) 1 .
- [31] S. Eidelmann et al., Review of Particle Physics, *Phys. Lett. B* 592 (2004) 1 ; <http://pdg.lbl.gov>.
- [32] S. Bethke, *J. Phys. G* 26 (2000) R27 .
- [33] G.M.Prospieri, M. Raciti and C.Simolo, in *this issue*.
- [34] T. van Ritbergen, J.A.M. Vermaseren, S.A. Larin, *Phys. Lett. B* 400 (1997) 379 .
- [35] W.A. Bardeen et al., *Phys. Rev. D* 18 (1978) 3998 .
- [36] K.G. Chetyrkin, B.A. Kniehl and M. Steinhauser, *Phys. Rev. Lett.* 79 (1997) 2184 .
- [37] W. Bernreuther and W. Wetzel, *Nucl. Phys. B* 197 (1982) 128 .
- [38] S.A. Larin, T. van Ritbergen and J.A.M. Vermaseren, *Nucl. Phys. B* 438 (1995) 278 .
- [39] S. Catani, L. Trentadue, G. Turnock, B.R. Webber, *Nucl. Phys. B* 407 (1993) 3 .
- [40] P.M. Stevenson, *Phys. Rev. D* 23 (1981) 2916 .
- [41] G. Grunberg, *Phys. Rev. D* 29 (1984) 2315 .
- [42] S.J. Brodsky, G.P. Lepage and P.B. Mackenzie, *Phys. Rev. D* 28 (1983) 228 .
- [43] S. Bethke, *Z. Phys. C* 43 (1989) 331 .
- [44] T. Sjostrand, *Comput. Phys. Commun.* 27 (1982) 243 .
- [45] T. Sjostrand, S. Mrenna and P Skands, hep-ph/0603175.
- [46] G. Marchesini and B.R. Webber, NPB 238 (1984) 1 ;
G. Corcella et al., *JHEP* 0101 (2001) 010 , hep-ph/0011363.
- [47] Yu.L. Dokshitzer, B.R. Webber, PLB 352 (1995) 451 ;
Yu.L. Dokshitzer, G. Marchesini, B.R. Webber, NPB 469 (1996) 93 ;
Yu.L. Dokshitzer, B.R. Webber, PLB 404 (1997) 321 ;
S. Catani, B.R. Webber, PLB 427 (1998) 377 ;
Yu.L. Dokshitzer, A. Lucenti, G. Marchesini, G.P. Salam, NPB 511 (1998) 296 ; *JHEP* 05 (1998) 003 .
- [48] P. Weisz, *Nucl. Phys. B (Proc. Suppl.)* 47 (1996) 71 ; hep-lat/9511017.
- [49] S. Bethke, Z. Kunszt, D.E. Soper, W.J. Stirling, *Nucl. Phys. B* 370 (1992) 310; erratum-ibid. B523 (1998) 681.
- [50] Yu. Dokshitzer, in *Workshop on Jet Studies at LEP and HERA, Durham 1990*; see *J. Phys. G* 17 (1991) 1572 ff;
N. Brown and W.J. Stirling, *Z. Phys. C* 53 (1992) 629.
- [51] S. Bethke, *Proc. of the 23rd Rencontre de Moriond: Current Issues in Hadron Physics, Les Arcs, France, 1988*, LBL-25247.
- [52] S. Bethke, *Nucl. Phys. Proc. Suppl.* 54A (1997) 314 , hep-ex/9609014.
- [53] M. Bengtsson and P.M. Zerwas, *Phys. Lett. B* 208 (1988) 306 .

- [54] L3 Collaboration, B. Adeva et al., *Phys. Lett. B* 248 (1990) 227.
- [55] S. Kluth, *Proc. 10th International QCD Conference (QCD 03)*, Montpellier, France, 2-9 Jul 2003; hep-ex/0309070.
- [56] ALEPH Collaboration, A. Heister et al., *Eur. Phys. J. C* 27 (2003) 1 .
- [57] DELPHI Collaboration, J. Abdallah et al. *Eur. Phys. J. C* 38 (2005) 413 ; hep-ex/0410071.
- [58] OPAL Collaboration, G. Abbiendi et al., hep-ex/0601048.
- [59] Z. Nagy and Z. Trócsányi, *Phys. Rev. D* 59 (1999) 14020 ; Erratum, *ibid.* 62 (2000) 099902 .
- [60] J. Schieck for the JADE collaboration, Contrib. to EPS Internat. Europhysics Conf. on High Energy Physics (HEP-EPS 2005), Lisbon, Portugal, 21-27 Jul 2005; hep-ex/0512004; to be submitted to *Eur. Phys. J. C*.
- [61] V.N. Gribov and L.N. Lipatov, *Sov. J. Nucl. Phys.* 15 (1972) 438 ; Yu.L. Dokshitzer, *Sov. Phys. JETP* 46 (1977) 641 .
- [62] G. Altarelli and G. Parisi, *Nucl. Phys. B* 126 (1977) 298 .
- [63] W. Furmanski and R. Petronzio, *Z. Phys. C* 11 (1982) 293 .
- [64] A. Vogt, S. Moch and J. Vermaseren, *Phys. Lett. B* 625 (2005) 245 .
- [65] M. Gluck, E. Reya, C. Schuck, hep-ph/0604116 (2006).
- [66] V. Chekelian, *Nucl. Phys. A* 755 (2005) 111 ; hep-ex/0502008.
- [67] C. Glasman, *AIP Conf.Proc.* 792 (2005) 689 , hep-ex/0506035.
- [68] S. Bethke and S. Catani, *Proc. of the XXVIIth Rencontre de Moriond*, Les Arcs, France, 1992; CERN-TH.6484/92.
- [69] S. Bethke, *Nucl.Phys.Proc.Suppl.* 135 (2004) 345 , hep-ex/0406058.
- [70] M. Davier, A. Höcker, Z. Zhang, hep-ph/0507078 (2005).
- [71] S. Bethke, *Phys. Rep.* 403-404 (2004) 203 ; hep-ex/0406058
- [72] S. Kluth, *Rept. Prog. Phys.* 69 (2006) 1771 ; hep-ex/0603011.
- [73] Q. Mason et al., *Phys. Rev. Lett.* 95 (2005) 052002 , hep-lat 0503005.
- [74] P. Weisz, private communication.
- [75] M. Schmelling, *Phys. Scripta* 51 (1995) 676 .
- [76] J. Blümlein and H. Böttcher, *Nucl. Phys. B* 636 (2002) 225 , hep-ph/0203155.
- [77] J. Ellis and M. Karliner, *Phys. Lett. B* 341 (1995) 397 .
- [78] CCFR Collaboration, J.H. Kim et al., *Phys. Rev. Lett.* 81 (1998) 3595 .
- [79] A.L. Kataev et al., hep-ph/0106221.
- [80] J. Santiago, F.J. Yndurain, hep-ph/0102247; *Nucl. Phys. B* 611 (2001) 447 .
- [81] S. Bethke, Proc. of the *QCD 02 High-Energy Physics International Conference in QCD*, Montpellier (France) July 2-9, 2002; hep-ex/0211012.
- [82] A. Penin, A.A. Pivovarov, *Phys. Lett. B* 435 (1998) 413 .
- [83] S. Albino et al., hep-ph/0205069; *Phys. Rev. Lett.* 89 (2002) 122004 .
- [84] CLEO Collaboration, R. Ammar et al., *Phys. Rev. D* 57 (1998) 1350 .
- [85] P.A. Movilla Fernandez, hep-ex/0205014.
- [86] D. Haidt, in *Directions in High Energy Physics* Vol 14, Precision Tests of the Standard Electroweak Model, ed. P. Langacker, World Scientific, 1995.
- [87] TOPAZ Collaboration, Y. Ohnishi et al. *Phys. Lett. B* 313 (1993) 475 .
- [88] UA1 Collaboration, C. Albajar et al., *Phys. Lett. B* 369 (1996) 46 .

- [89] UA6 Collaboration, M. Werlen et al., *Phys. Lett. B* 452 (1999) 201 .
- [90] T. Affolder et al., CDF collaboration, hep-ex/0108034; *Phys. Rev. Lett.* 88 (2002) 042001 .
- [91] The LEP Collaborations ALEPH, DELPHI, L3 and OPAL; hep-ex/0509008.
- [92] *this review*.
- [93] M. Klasen, *AIP Conf. Proc.* 792 (2005) 681 , hep-ph/0506252.
- [94] W. de Boer and C. Sander, *Phys. Lett. B* 585 (2004) 276 , hep-ph/0307049.
- [95] G.A. Blair et al., hep-ph/0512084.

Table 1: World summary of measurements of α_s (status of April 2006): DIS = deep inelastic scattering; GLS-SR = Gross-Llewellyn-Smith sum rule; Bj-SR = Bjorken sum rule; (N)NLO = (next-to-)next-to-leading order perturbation theory; LGT = lattice gauge theory; resum. = resummed NLO. New or updated entries since the review of 2004 [69] are underlined.

Process	Q [GeV]	$\alpha_s(Q)$	$\alpha_s(M_{Z^0})$	$\Delta\alpha_s(M_{Z^0})$		Theory	refs.
				exp.	theor.		
DIS [pol. SF]	0.7 - 8		$0.113 \pm^{+0.010}_{-0.008}$	± 0.004	$^{+0.009}_{-0.006}$	NLO	[76]
DIS [Bj-SR]	1.58	$0.375 \pm^{+0.062}_{-0.081}$	$0.121 \pm^{+0.005}_{-0.009}$	–	–	NNLO	[77]
DIS [GLS-SR]	1.73	$0.280 \pm^{+0.070}_{-0.068}$	$0.112 \pm^{+0.009}_{-0.012}$	$^{+0.008}_{-0.010}$	0.005	NNLO	[78]
<u>τ-decays</u>	1.78	0.345 ± 0.010	0.1215 ± 0.0012	0.0004	0.0011	NNLO	[70]
DIS [ν ; xF_3]	2.8 - 11		$0.119 \pm^{+0.007}_{-0.006}$	0.005	$^{+0.005}_{-0.003}$	NNLO	[79]
DIS [e/μ ; F_2]	2 - 15		0.1166 ± 0.0022	0.0009	0.0020	NNLO	[80, 81]
DIS [e -p \rightarrow jets]	6 - 100		0.1186 ± 0.0051	0.0011	0.0050	NLO	[67]
Υ decays	4.75	0.217 ± 0.021	0.118 ± 0.006	–	–	NNLO	[82]
<u>QQ states</u>	7.5	0.1886 ± 0.0032	0.1170 ± 0.0012	0.0000	0.0012	LGT	[73]
<u>e^+e^- [F_2^{γ}]</u>	1.4 - 28		$0.1198 \pm^{+0.0044}_{-0.0054}$	0.0028	$^{+0.0034}_{-0.0046}$	NLO	[83]
e^+e^- [σ_{had}]	10.52	0.20 ± 0.06	$0.130 \pm^{+0.021}_{-0.029}$	$^{+0.021}_{-0.029}$	0.002	NNLO	[84]
e^+e^- [jets & shps]	14.0	$0.170 \pm^{+0.021}_{-0.017}$	$0.120 \pm^{+0.010}_{-0.008}$	0.002	$^{+0.009}_{-0.008}$	resum	[85]
e^+e^- [jets & shps]	22.0	$0.151 \pm^{+0.015}_{-0.013}$	$0.118 \pm^{+0.009}_{-0.008}$	0.003	$^{+0.009}_{-0.007}$	resum	[85]
e^+e^- [jets & shps]	35.0	$0.145 \pm^{+0.012}_{-0.007}$	$0.123 \pm^{+0.008}_{-0.006}$	0.002	$^{+0.008}_{-0.005}$	resum	[85]
e^+e^- [σ_{had}]	42.4	0.144 ± 0.029	0.126 ± 0.022	0.022	0.002	NNLO	[86, 32]
e^+e^- [jets & shps]	44.0	$0.139 \pm^{+0.011}_{-0.008}$	$0.123 \pm^{+0.008}_{-0.006}$	0.003	$^{+0.007}_{-0.005}$	resum	[85]
e^+e^- [jets & shps]	58.0	0.132 ± 0.008	0.123 ± 0.007	0.003	0.007	resum	[87]
$p\bar{p} \rightarrow b\bar{b}X$	20.0	$0.145 \pm^{+0.018}_{-0.019}$	0.113 ± 0.011	$^{+0.007}_{-0.006}$	$^{+0.008}_{-0.009}$	NLO	[88]
$p\bar{p}, pp \rightarrow \gamma X$	24.3	$0.135 \pm^{+0.012}_{-0.008}$	$0.110 \pm^{+0.008}_{-0.005}$	0.004	$^{+0.007}_{-0.003}$	NLO	[89]
$\sigma(p\bar{p} \rightarrow \text{jets})$	40 - 250		0.118 ± 0.012	$^{+0.008}_{-0.010}$	$^{+0.009}_{-0.008}$	NLO	[90]
$e^+e^- \Gamma(Z \rightarrow \text{had})$	91.2	$0.1226 \pm^{+0.0058}_{-0.0038}$	$0.1226 \pm^{+0.0058}_{-0.0038}$	± 0.0038	$^{+0.0043}_{-0.0005}$	NNLO	[91]
<u>e^+e^- 4-jet rate</u>	91.2	0.1176 ± 0.0022	0.1176 ± 0.0022	0.0010	0.0020	NLO	[92]
e^+e^- [jets & shps]	91.2	0.121 ± 0.006	0.121 ± 0.006	0.001	0.006	resum	[32]
e^+e^- [jets & shps]	133	0.113 ± 0.008	0.120 ± 0.007	0.003	0.006	resum	[32]
e^+e^- [jets & shps]	161	0.109 ± 0.007	0.118 ± 0.008	0.005	0.006	resum	[32]
e^+e^- [jets & shps]	172	0.104 ± 0.007	0.114 ± 0.008	0.005	0.006	resum	[32]
e^+e^- [jets & shps]	183	0.109 ± 0.005	0.121 ± 0.006	0.002	0.005	resum	[32]
e^+e^- [jets & shps]	189	0.109 ± 0.004	0.121 ± 0.005	0.001	0.005	resum	[32]
e^+e^- [jets & shps]	195	0.109 ± 0.005	0.122 ± 0.006	0.001	0.006	resum	[81]
e^+e^- [jets & shps]	201	0.110 ± 0.005	0.124 ± 0.006	0.002	0.006	resum	[81]
e^+e^- [jets & shps]	206	0.110 ± 0.005	0.124 ± 0.006	0.001	0.006	resum	[81]

Table 2: Measurements of $\alpha_s(M_{Z^0})$ included in the process to determine the world average, c.f. table 1. The rightmost two columns give the exclusive mean value of $\alpha_s(M_{Z^0})$ calculated *without* that particular measurement, and the number of standard deviations between this measurement and the respective exclusive mean, treating errors as described in the text. The inclusive average from *all* listed measurements gives $\alpha_s(M_{Z^0}) = 0.1189 \pm 0.0007$.

Process	Q [GeV]	$\alpha_s(M_{Z^0})$	excl. mean $\alpha_s(M_{Z^0})$	std. dev.
DIS [Bj-SR]	1.58	$0.121 \begin{smallmatrix} + 0.005 \\ - 0.009 \end{smallmatrix}$	0.1189 ± 0.0008	0.3
τ -decays	1.78	0.1215 ± 0.0012	0.1176 ± 0.0018	1.8
DIS [ν ; $x F_3$]	2.8 - 11	$0.119 \begin{smallmatrix} + 0.007 \\ - 0.006 \end{smallmatrix}$	0.1189 ± 0.0008	0.0
DIS [e/μ ; F_2]	2 - 15	0.1166 ± 0.0022	0.1192 ± 0.0008	1.1
DIS [e-p \rightarrow jets]	6 - 100	0.1186 ± 0.0051	0.1190 ± 0.0008	0.1
Υ decays	4.75	0.118 ± 0.006	0.1190 ± 0.0008	0.2
$Q\bar{Q}$ states	7.5	0.1170 ± 0.0012	0.1200 ± 0.0014	1.6
$e^+e^- [\Gamma(Z \rightarrow had)]$	91.2	$0.1226 \begin{smallmatrix} + 0.0058 \\ - 0.0038 \end{smallmatrix}$	0.1189 ± 0.0008	0.9
e^+e^- 4-jet rate	91.2	0.1176 ± 0.0022	0.1191 ± 0.0008	0.6
e^+e^- [jets & shps]	189	0.121 ± 0.005	0.1188 ± 0.0008	0.4